GA–A20911
UC–224

TFE VERIFICATION PROGRAM

SEMIANNUAL REPORT FOR THE PERIOD ENDING MARCH 31, 1992

Prepared under
CONTRACT DE-AC03-86SF16298
FOR THE SAN FRANCISCO OPERATIONS OFFICE
DEPARTMENT OF ENERGY

DATE PUBLISHED: APRIL 1992

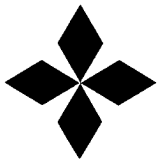

GENERAL ATOMICS

DISCLAIMER

This report has been reproduced directly from the best available copy.

Available to DOE and DOE contractors from the Office of Scientific and Technical Information, P.O. Box 62, Oak Ridge, TN 37831; prices available from (615) 576-8401, FTS 626-8401.

Available to the public from the National Technical Information Service, U.S. Department of Commerce, 5285 Port Royal Rd., Springfield, VA 22161.

Accession Number: 4387

Publication Date: Apr 01, 1992

Title: TFE Verification Program, Semiannual Report for period ending March 31, 1992

Corporate Author Or Publisher: General Atomics, P.O. Box 85608, San Diego, Ca 92186-9784 Report Number: GA-A20911

Report Prepared for: San Francisco Operations Office, Department of Energy

Descriptors, Keywords: TFE Verification General Atomics Semiannual Report Energy

Pages: 00085

Cataloged Date: Mar 18, 1993

Document Type: HC

Number of Copies In Library: 000001

Record ID: 26463

GA-A20911
UC-224

TFE VERIFICATION PROGRAM

SEMIANNUAL REPORT
FOR THE PERIOD ENDING MARCH 31, 1992

Prepared under
CONTRACT DE-AC03-86SF16298
FOR THE SAN FRANCISCO OPERATIONS OFFICE
DEPARTMENT OF ENERGY

GENERAL ATOMICS PROJECT NO. 3450
DATE PUBLISHED: APRIL 1992

GENERAL ATOMICS

CONTENTS

CONTENTS

FIGURES

TABLES

1. INTRODUCTION

1.1 OBJECTIVE OF PROGRESS REPORT

The objective of the semiannual progress report is to summarize the technical results obtained during the latest reporting period. The information presented herein will include evaluated test data, design evaluations, the results of analyses and the significance of results.

1.2 TFE VERIFICATION PROGRAM GOAL

The program objective is to demonstrate the technology readiness of a TFE suitable for use as the basic element in a thermionic reactor with electric power output in the 0.5 to 5.0 MW(e) range, and a full-power life of 7 years.

1.3 TECHNICAL APPROACH

The TFE Verification Program builds directly on the technology and data base developed in the 1960s and early 1970s in an AEC/NASA program, and in the SP-100 program conducted in 1983, 1984 and 1985. In the SP-100 program, the attractive features of thermionic power conversion technology were recognized but concern was expressed over the lack of fast reactor irradiation data. The TFE Verification Program addresses this concern.

The general logic and strategy of the program to achieve its objectives is shown on Fig. 1-1. Five prior programs form the basis for the TFE Verification Program:

1) AEC/NASA program of the 1960s and early 1970s.
2) SP-100 concept development program.
3) SP-100 thermionic technology program.
4) Thermionic irradiations program in TRIGA in FY-86.
5) Thermionic Technology Program in 1986 and 1987.

These programs provide both the systems and technology expertise necessary to design and demonstrate a megawatt class TFE.

Figure 1-1

LOGIC TO DEMONSTRATE TECHNOLOGY READINESS OF MEGAWATT CLASS TFE

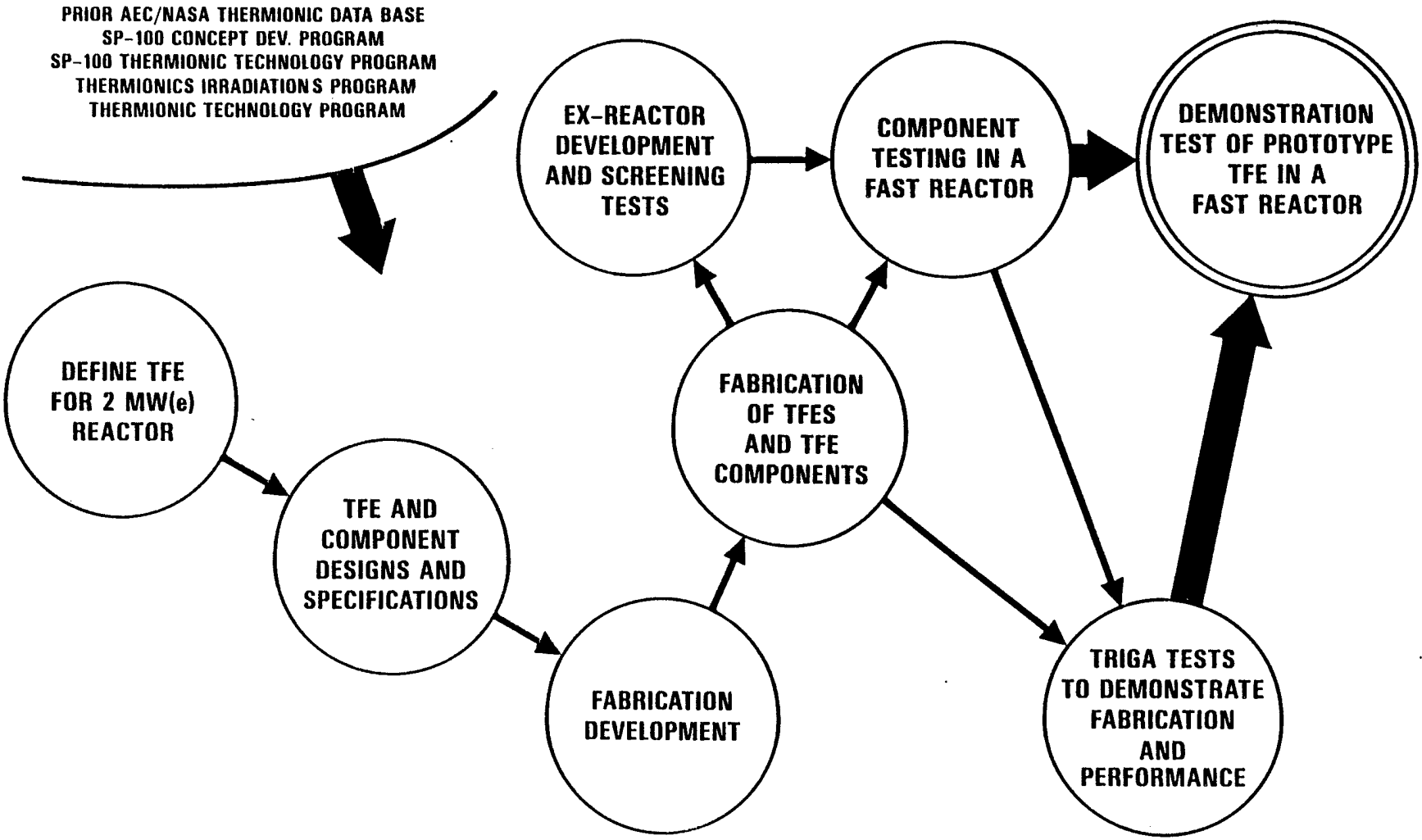

The approach to be followed is to design a TFE that will meet the reliability and lifetime requirements for the 2 MW(e) conceptual reactor design, and initiate component testing in a fast reactor. The demonstration of a 7-year component lifetime capability will be through the combined use of analytical models and accelerated, confirmatory tests. Iterative testing will be performed where the results of one test series will lead to evolutionary improvements in the next test specimens.

The TFE components will undergo screening and initial development testing in ex-reactor tests. Several design and materials options will be considered for each component. As screening tests permit, down selection will occur. It is necessary to rapidly make baseline design and materials selections to make optimum use of irradiation testing.

In parallel with ex-reactor testing, and fast reactor component testing, components will be integrated into a TFE and tested in the TRIGA. Realtime testing of partial length TFEs will be used to test support, alignment and interconnective TFE components, and to verify TFE performance in-reactor with integral cesium reservoirs. Realtime testing will also be used to verify the relation between TFE performance and fueled emitter swelling, to test the durability of intercell insulation, to check temperature distributions, and to verify the adequacy over time of the fission gas venting channels.

Predictions of TFE lifetime will rest primarily on the accelerated component testing results, as correlated and extended to realtime by the analytical models developed.

The fast reactor testing of fueled emitters will be calibrated by verifying the accuracy of emitter temperature predictions through complementary analysis and ex-reactor and in-reactor diagnostic tests. Instrumented sheath insulators will be tested in a fast reactor with an applied voltage.

A test of prototypic TFEs will be run in a fast reactor as a verification of the basic TFE design. This design may be upgraded based on the final component testing results.

The deliverables of the program are:

1) Conceptual design of a megawatt class power system including component specifications and a system description.
2) Thermionic components with verified performance.
3) TFE demonstration in a fast reactor.
4) Fabrication process specifications.
5) Verified performance models.

2. CONCEPT DESIGN TASK

2.1 OBJECTIVE

Task 2 provides the design guidance for the TFE Verification Program. The primary goals of this task are:

1) Establish the conceptual design of an in-core thermionic reactor for a 2 MW(e) space nuclear power system with a 7-year operating lifetime.
2) Demonstrate scalability of the above concept over the output power range of 500 kW(e) to 5 MW(e).
3) Define the TFE which is the basis for the 2 MW(e) reactor design. This TFE specification will then be the basis for the test program.

2.2 TECHNICAL APPROACH

The technical approach being taken in the concept design effort can be characterized as follows:

1) Perform system-level tradeoffs to determine initial TFE features and reactor scalability trends;
2) Refine these results and identify the 2 MW(e) reactor general arrangement with primary emphasis on characterizing the features and performance of the TFE;
3) Enter this information into the program data base via two separate design description documents:
    - o Two MW(e) reactor-converter system description.
    - o TFE component specification.

2.3 SYSTEM DEFINITION UPDATE

The current description of the 2 MW(e) thermionic power system used to define the reference TFE for the program is shown on Table 2.1. This has not changed during the current reporting period.

TABLE 2-1

TFE DESIGN DEFINITION

PERFORMANCE	
Overall TFE:	
Output electrical power (We)	662
Efficiency	9.3
Maximum voltage	5.9 (15)
U-235 burnup (a/o)	4.1 avg, 5.3 peak
Fluence (nvt)	2.7×10^{22} avg, 3.5×10^{22} peak
Converter:	
Converter power (Wt/We)	594/55.2
Emitter power flux (We/cm^2)	2.72
Diode current density (a/cm^2)	7.0
Thermionic work function (eV)	4.9
Emitter temperature (K)	1800
Collector temperature (K)	1000
Cesium pd (mil-torr)	30
Converter output voltage	0.49
Converter current (amp)	140
CONFIGURATION	
Overall TFE:	
TFE length (active core) (in)	39.6
TFE length (overall)	TBD
Sheath tube o.d. (in)	0.694
Lead o.d. (in)	0.875
Lead length (in)	4
Converters per TFE	12
Converter:	
Emitter o.d. x L x t (in)	0.52 x 2.0 x 0.040
Emitter stem L x t (in)	0.45 x 0.020
Diode gap (in)	0.010
Trilayer t: collector	0.028
insulator (in)	0.016
outer cylinder	0.028
Fuel specification	93% enriched UO_2; variable volume fraction
Intercell axial space (in)	0.74

3. CONVERTER PERFORMANCE TASK

3.1 OBJECTIVE

The objective of the converter performance task is to establish accurate converter performance models which have been correlated to observe test data. The data base will be developed from near prototypic converters using emitter and collector materials of interest over the full range of anticipated operating parameters. Part of the data base will include off-design and non-ideal operation of the converters. The resulting models will be used to determine the optimum converter configuration (materials, additives, spacing, etc.) for use in the prototypic TFE and reactor design.

A thermionic reactor is composed of a large array of thermionic cells, each of which has a unique input power, emitter temperature, and operating current density. In addition, individual cells will vary in performance over the system lifetime due to changing operating conditions caused by fuel burnup and variations in operating power requirement, or losses of some of the cells. Thus, the design and performance prediction of a thermionic reactor require an extensive data base on prototypical cell performance over a wide range of operating conditions.

The data and models will also be used in the startup of the TFEs in TRIGA and the FFTF and also in the startup of thermionic reactors. The observed current-voltage data during startup can be related to system temperatures through the ex-reactor correlations.

3.2 TASK DESCRIPTION

The current test matrix is shown on Tables 3-1 and 3-2.

Planar Converter-1 (PC-1) is a planar (variable spacing) converter with a tungsten <110> emitter, a niobium collector and a graphite cesium reservoir external to the converter. The emitter has a small cavity for accepting a fuel pellet of depleted uranium oxide. The converter designation with the UO_2 pellet in the converter is PC-1 (MOD).

The original test strategy was to obtain performance maps without the UO_2, then add the UO_2 into the cavity and begin a life test. The effect of oxygen diffusion to the electrode surfaces could then be measured.

The revised test strategy is to build PC-1 (MOD) with the UO_2 in place. The initial performance maps would be characteristic of a thermionic device with no oxygen on the electrode surfaces. The subsequent life test would then show the effects of oxygen diffusion.

Background information on the PC-1 (MOD) experiment was presented in the last semiannual report (Ref. 3-1) and in Ref. 3-2. The current status of the effort is described below.

TABLE 3-1

EX-REACTOR PLANAR CONVERTER TEST PROGRAM

	Emitter	Collector	Cs Reservoir	Rationale for Test
PC-1	Duplex W*	Nb	Graphite	Performance map with graphite-cesium reservoir.
PC-2	Duplex W	Nb tilted	Pool	A verification of the model which relates converter output to emitter distortion
PC-3	High Strength Emitter	Nb	Pool	Establish data base on performance with high strength emitter
PC-1 (MOD)	Duplex W*	Nb	Graphite	UO_2 in contact with the emitter. Differential data on the UO_2 effect will be obtained during a life test.

*To be combined into one experiment to be designated PC-1 (MOD).

TABLE 3-2
EX-REACTOR CYLINDRICAL CONVERTER TEST PROGRAM

	Emitter	Collector	Reservoir	Life Test	Rationale for Test
CC-1	Duplex W	Nb	Graphite	No	Performance map with reference electrodes and reservoir

3.3 STATUS OF FABRICATION

Emitter fabrication was completed and the emitter assembly bonded. The graphite reservoir was outgassed, and final assembly was underway on March 1, 1992.

The test procedure which will be followed is as follows:

- o Outgas converter
- o Distill cesium into drum
- o Distill cesium from drum to reservoir
- o Pinch-off drum
- o Test PC-1(MOD) with cesium reservoir only
- o Open pinch-open device to graphite reservoir
- o Load graphite with cesium
- o Close cesium valve
- o Test PC-1(MOD) with cesium-graphite reservoir
- o Pinch-off cesium reservoir
- o Ship to Rasor Associates for life testing.

The test parameters are shown below:

	High	Low	Increment
Emitter Temperature (K)	2000	1600	100
Collector Temperature (K)	1100	600	100
Interelectrode Spacing (mm)	.5	.125	.025
Cesium Pressure (torr)	8	.5	Factor of 2

References

3-1 TFE Verification Program Semiannual Report for the Period Ending September 30, 1991; GA-A20804, Issued December 1991.

3-2 Miskolczy, G., D. Lieb and G. L. Hatch, "Design of a Planar Thermionic Converter to Measure the Effect of Diffusion of Uranium Oxide on Performance", Ninth Symposium on Space Power Systems, Albuquerque, NM, January 1992.

4. INSULATOR SEAL TASK

4.1 OBJECTIVE AND TECHNICAL APPROACH

The overall objective of the insulator seal task is to develop and validate the performance of an insulator seal for use in the thermionic fuel element reference design. In particular, the objectives are:

1. Produce designs for the insulator seal.
2. Develop required fabrication processes for the insulator seals designed and document the process specifications.
3. Fabricate insulator seals for ex-reactor and in-reactor testing.
4. Verify the performance characteristics and lifetimes associated with insulator seals by means of ex-reactor and in-reactor testing. Perform postirradiation examination of the seal specimens and use the test results to improve the seal design.
5. Develop an analytical model of the performance and lifetime of the insulator seal and validate the model with test data.

The insulator seal, shown schematically in Fig. 4-1, must provide electrical isolation between adjacent collectors while maintaining a leak-tight seal separating the cesium vapor of the interelectrode space from the fission products. The current design requirements are listed below:

1.	Insulator temperature	1070 to 1150 K
2.	Nominal fast fluence, E>0.1 MeV	2.3×10^{22} n/cm^2
3.	Nominal applied voltage	0.49 volts
	Maximum applied voltage	0.63 volts
4.	Operating environment	1-3 torr Cs and fission gases
5.	Leak tightness	$< 2 \times 10^{-11}$ std cc/s (fabricated)
		$< 5 \times 10^{-5}$ std cc/s (end lifetime)
6.	Electrical resistance	>10 ohms (1150 K)
7.	Lifetime	$\geq$ 7 years

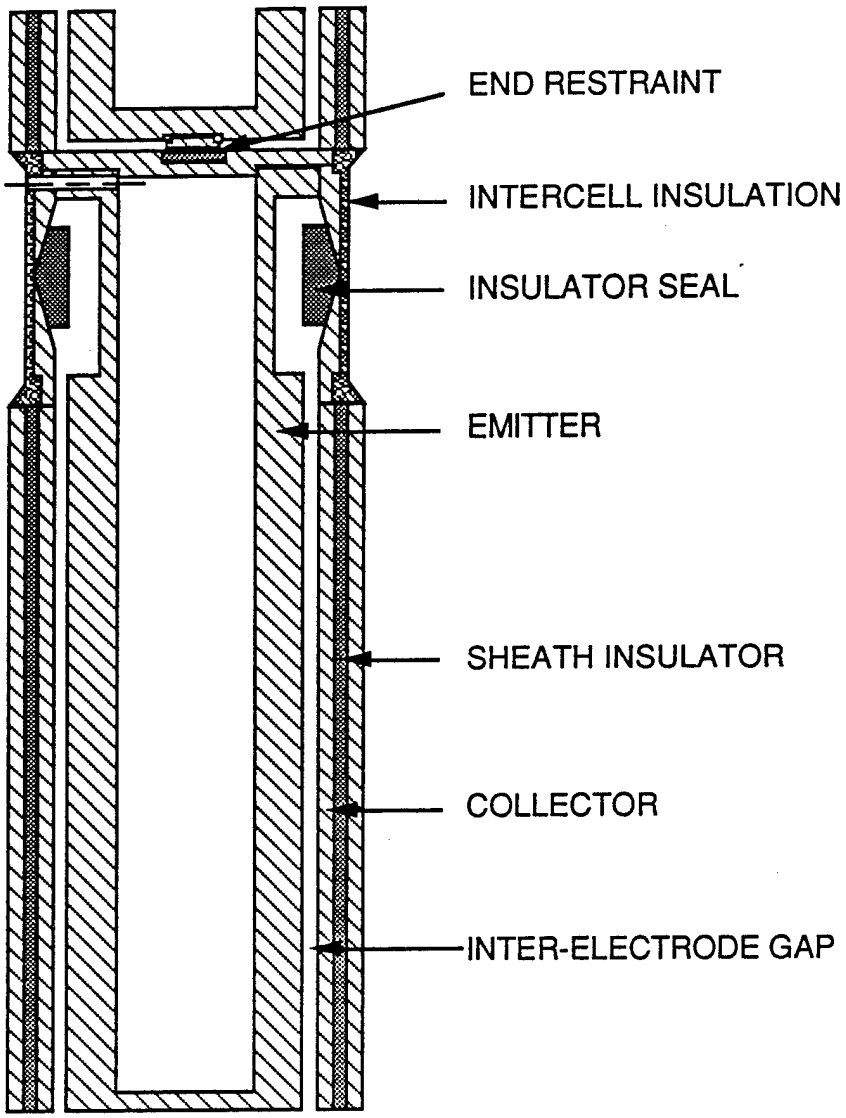

Figure 4-1 - Thermionic cell showing insulator locations

4.2 TASK DESCRIPTION

The insulator seal task consists of five subtasks:

1. Seal design. Seal designs consistent with the TFE requirements are to be developed. Designs being considered are the taper seal, the butt seal and trilayer seal.

2. Fabrication development. Select appropriate insulator materials. Develop appropriate bonding techniques for each insulator material selected. Fabricate sufficient insulator seal specimens to support the ex-reactor and in-reactor test effort. Prepare and issue process specifications. Insulator materials considered are alumina (Al_2O_3), yttria (Y_2O_3), and YAG ($Y_3Al_5O_{12}$).

3. Ex-reactor testing. Perform ex-reactor tests to evaluate the effects of thermal cycling, cesium compatibility, applied voltage and material interdiffusion on insulator seal performance and lifetime.

4. In-reactor testing. Perform in-reactor tests and the related post-irradiation examinations to determine seal mechanical stability, electrical resistance and hermeticity after exposure to fast neutron fluences.

5. Modeling. Develop and validate analytical models to predict seal lifetime and performance.

4.3 DESIGN AND MATERIALS DOWNSELECTION

The seal design has been downselected to the taper and trilayer configurations as shown in Fig. 4-2. The trilayer design is similar in technology to the sheath

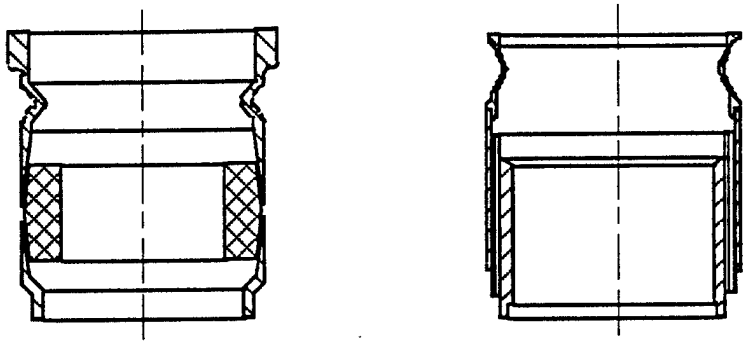

Figure 4-2. Insulator seal designs

insulator (Task 5). The insulator materials used for the taper seal are single crystal alumina, polycrystalline alumina and polycrystalline YAG. PIE results of the UCA-2 single crystal YAG taper seal shows that YAG has good neutron damage resistance and require additional testing. YAG exhibits considerably less swelling than alumina but is not as strong. The insulator material selected for the trilayer seal is alumina in either the graded or cermet configurations.

4.4 EX-REACTOR TESTING

A 5% niobium cermet trilayer insulator seal was tested for 82 days at 1273 K and 1 volt. The resistivity of the sample remained constant in the range of 3 to $5x10^8$ ohms-cm. Testing was stopped due to failure in the vacuum system as a result of a malfunctioning turbo pump. Since the vacuum failure occurred when the sample was at temperature the sample was badly oxidized and had to be removed from the test stand. A new cermet trilayer insulator seal with 10% niobium was installed. This trilayer seal is from the same batch of seals fabricated for the UCA-3 test. The activation energy for electrical conduction was measured and has a value of 2.7 eV in the temperature range 970 K to 1420 K. The sample is being tested at 1273 K and 1 volt. The resistivity as a function of time for the last 30 days has remained constant in the range of 4 to $6x10^8$ ohm-cm.

4.5 IN-REACTOR TESTING

4.5.1 UCA-3 Irradiation

UCA-3 is the most recent experiment in the series of in-reactor component testing. It incorporates results from ex-reactor testing as well as results from the postirradiation examination of UCA-1 and UCA-2 insulator seals. The UCA-3 test consists of two batches. Irradiation of Batch-A started in cycle 156 of EBR-II in December 1990 and ended in March 1991 with a total of 95 EFPD and an estimated

peak fast fluence of 1.5×10^{22} n/cm^2 (E>.1 MeV). Batch-B was irradiated in cycles 157 and 158 of EBR-II with irradiation ending on January 19, 1992. Batch B samples accumulated a total of 110 EFPD with an estimated peak fast fluence of 1.8×10^{22} n/cm^2 (E>.1 MeV). The Batch-B capsules are in the process of thermal cooldown at EBR-II. Disassembly of the capsule and neutron radiography is scheduled for March 1992. Both Batch-A and -B will be shipped to WHC in April for postirradiation examination. Shown in Table 4-1 is the UCA-3 sample test matrix.

TABLE 4-1

UCA-3 INSULATOR SEALS TEST MATRIX

Materials	Batch	Configuration	Number
Alumina (SC)	A	Taper	2
Alumina (SC)	B	Taper	2
YAG (PC)	B	Taper	1
Alumina (PC)	B	Trilayer graded	2
Alumina (PC)	B	Trilayer cermet 5% Nb	2
Alumina (PC)	B	Trilayer cermet 10% Nb	2

SC - Single crystal
PC - Polycrystalline

4.6 STATUS SUMMARY

The current reference insulator seal specifications are summarized below:

Reference material: Single crystal Al_2O_3

Design: Taper seal

Fabrication: Braze to niobium.

The insulator material backups are:

Polycrystalline YAG

Polycrystalline alumina.

The seal design backup is:

Alumina trilayer either graded or cermet.

The polycrystalline alumina taper seal has experienced over 30,000 real time test hours in the TRIGA reactor, good evidence that its lifetime is at least several years. YAG is also being carried as a backup because of its low irradiation induced swelling and good electrical properties. More fabrication development and testing, both in-reactor and ex-reactor, are needed for YAG.

The alumina trilayer design used in the sheath insulator task (Task 5) has remained hermetic after irradiation to three times the nominal fluence expected for the insulator seals. The trilayer design is being carried as an alternate in case the taper seal cannot be made leak tight.

Table 4-2 summarizes the seal development effort so far.

References

4-1 TFE Verification Program Semiannual Report for the Period Ending September 30, 1991, GA-A20804.

Table 4-2
INSULATOR SEAL DEVELOPMENT EFFORT

Material	Design	Electrical Properties	Neutron Stability	Fabricability	Test Matrix (No. of Specimens)					
					UCA-1	UCA-2	UFAC-3	UCA-3	TFE 1H1, 1H2, 1H3, 3H1, 3H5, 6H1	Fueled Emitter
Alumina	Taper SC	Good	Acceptable	Good	3	1	1	4		
YAG	Taper SC	Acceptable	Good	Good		1				
Alumina	Taper PC	Good	Acceptable	Good					19	9
YAG	Taper PC	Good	Good	Good			3	1		
Alumina	Trilayer Graded	Good	Acceptable	Good	6	2		2		
Alumina	Trilayer Cermet	Good	Good	Good	3	2		4		

PC Polycrystalline
SC Single crystal

5. SHEATH INSULATOR TASK

5.1 OBJECTIVE AND TECHNICAL APPROACH

The overall objective of the sheath insulator task is to develop and validate the performance of a sheath insulator for use in the TFE reference design. In particular, the objectives are:

1. Produce designs for the sheath insulator.
2. Develop required fabrication processes for the sheath insulators designed and document the process specifications.
3. Fabricate sheath insulators for ex-reactor and in-reactor (uninstrumented and instrumented) testing.
4. Verify the performance characteristics and lifetimes associated with sheath insulators by means of ex-reactor and in-reactor testing.
5. Develop an analytical model of the performance and lifetime of the sheath insulator and validate the model with test data.

The sheath insulator, shown schematically in Fig. 5-1, must provide electrical isolation between the collector of each converter and the outer sheath tube. The outer sheath tube is in contact with the reactor liquid metal coolant. The sheath insulator must also provide good thermal conduction between the collector and the sheath tube. The current design requirements are listed below:

1.	Insulator temperature	1070 K
2.	Nominal fast fluence, E>0.1 MeV	2.3×10^{22} n/cm^2
3.	Nominal applied voltage	5.9 volts
	Maximum applied voltage	7.5 volts
4.	Operating environment	Fission gases
5.	Electrical resistance	>1000 ohms (1070 K)
6.	Thermal conductivity	>0.03 W/cm-K)
7.	Lifetime	$\geq$ 7 years

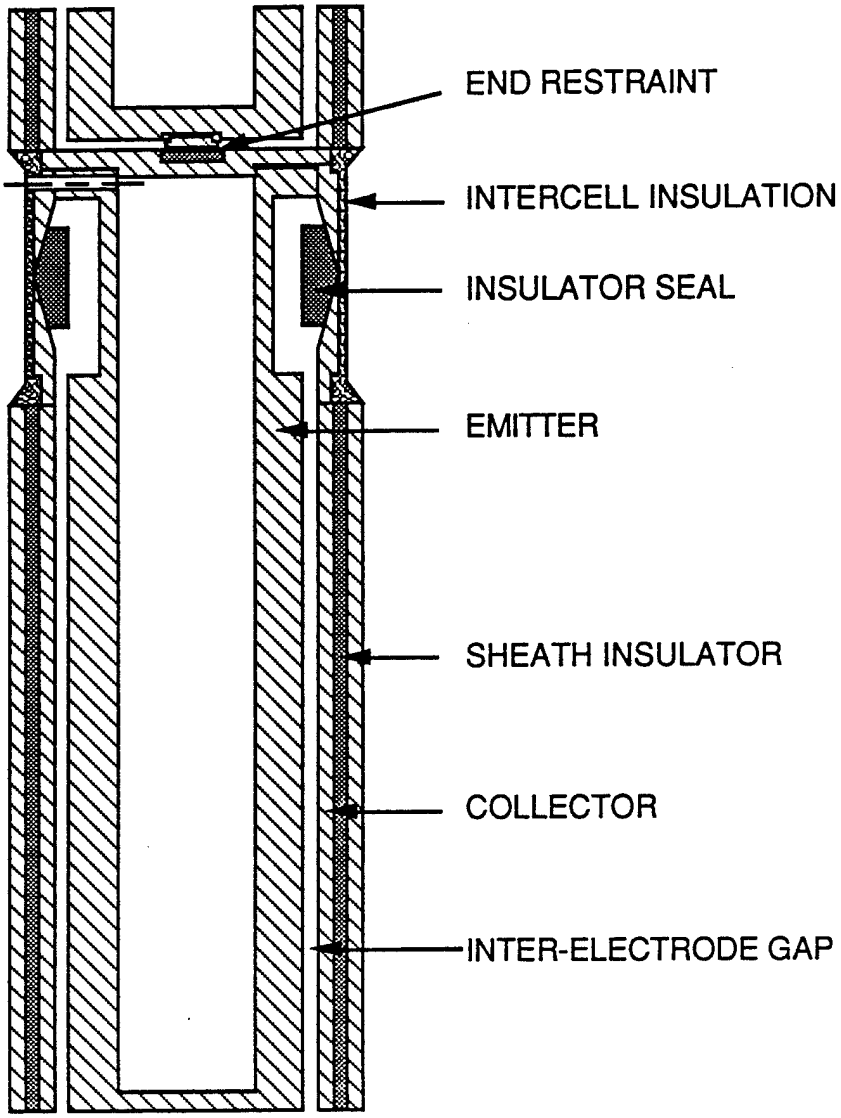

Figure 5-1. Thermionic cell showing insulator locations

The technical concerns are the unbonding of the sheath insulator structure due to fast neutron induced damage, and electrolysis that could lead to low electrical resistance, and electrical breakdown. The objective of the sheath insulator task is to resolve these concerns and to develop and validate the performance of a sheath insulator for use in a prototypic TFE.

5.2 TASK DESCRIPTION

The sheath insulator task consists of five subtasks:

1. Sheath design. Sheath designs consistent with the TFE requirements are to be developed. The current design is the trilayer, consisting of an insulator between the niobium collector and the outer niobium sheath tube.
2. Fabrication development. Select appropriate insulator materials. Develop appropriate fabrication techniques for each insulator material selected. Fabricate sufficient sheath insulator specimens to support the ex-reactor and in-reactor test efforts. Prepare and issue process specifications. Insulator materials being considered are alumina (Al_2O_3), yttria (Y_2O_3), and YAG ($Y_3Al_5O_{12}$). The fabrication techniques include plasma spraying the insulator onto the niobium collector, and thermal bonding of free standing ceramic tubes to the collector.
3. Ex-reactor testing. Perform ex-reactor tests to evaluate the effects of thermal cycling, applied voltage and material interdiffusion on the sheath insulators performance and lifetime.
4. In-reactor testing. Perform uninstrumented and instrumented in-reactor tests and the related postirradiation examinations. Determine the sheath insulator mechanical stability, electrical resistance and thermal conductivity after exposure to fast neutron fluence with and without an applied voltage.
5. Modeling. Develop and validate analytical models to predict sheath insulator lifetime and performance.

5.3 DESIGN AND MATERIALS

Two manufacturing processes and one insulator material are currently being evaluated. The manufacturing processes are the plasma sprayed graded trilayer being developed at GA and the cermet trilayer being developed at Thermo Electron Technologies (TTC). The insulator material under investigation is aluminum oxide.

5.4 EX-REACTOR TESTING

Rasor Associates, Inc. (RAI) performs all the ex-reactor testing of the sheath insulators. Tests include long term tests at the nominal operating temperature (1070 K) and applied potential (7.5 volts), and accelerated tests at higher temperatures (1170 K and 1270 K) and higher applied potentials (30, 50 and 100 volts).

A FY-91 sheath insulator batch is currently being tested at RAI. Nine of the twelve samples are from the same fabrication batch as the UCA-3 Batch B sheath insulators that were tested at EBR-II. The sample batch consists of three graded alumina sheaths made with Linde A alumina (UCA-3), three graded sheaths made with Linde B alumina, three alumina cermet sheaths made with 5% niobium powder (UCA-3) and three alumina cermet sheaths made with 10% niobium powder (UCA-3). One sample of each type is being tested at the nominal TFE operating temperature of 1070 K and at the accelerated temperatures of 1170 K and 1270 K.

The samples were tested for 90 days with an applied potential of 7.5 volts and showed a stable performance as function of temperature and time. The applied potential was then increased to 100 volts (accelerated condition). Several days after the voltage was increased two of the 10% niobium cermets shorted out. These two cermets were being tested at the higher temperatures. The samples were removed from the test stand because they were affecting the electrical behavior of some of the other samples. The remaining 10 samples have been tested for a total of 259 days, the last 169 days at 100 volts.

Results of the resistivity as a function of time, temperature, and voltage is shown in Figs. 5-2, 5-3, 5-4 and 5-5 for the graded Linde A, graded Linde B, 5% niobium cermet, and 10% niobium cermet samples respectively. Samples 1685, 1687 and 1707 C have high resistivity at the test temperature but they are exhibiting a small temperature dependence during the weekly temperature scans. The small temperature dependence started after the two 10% niobium cermets failed. The

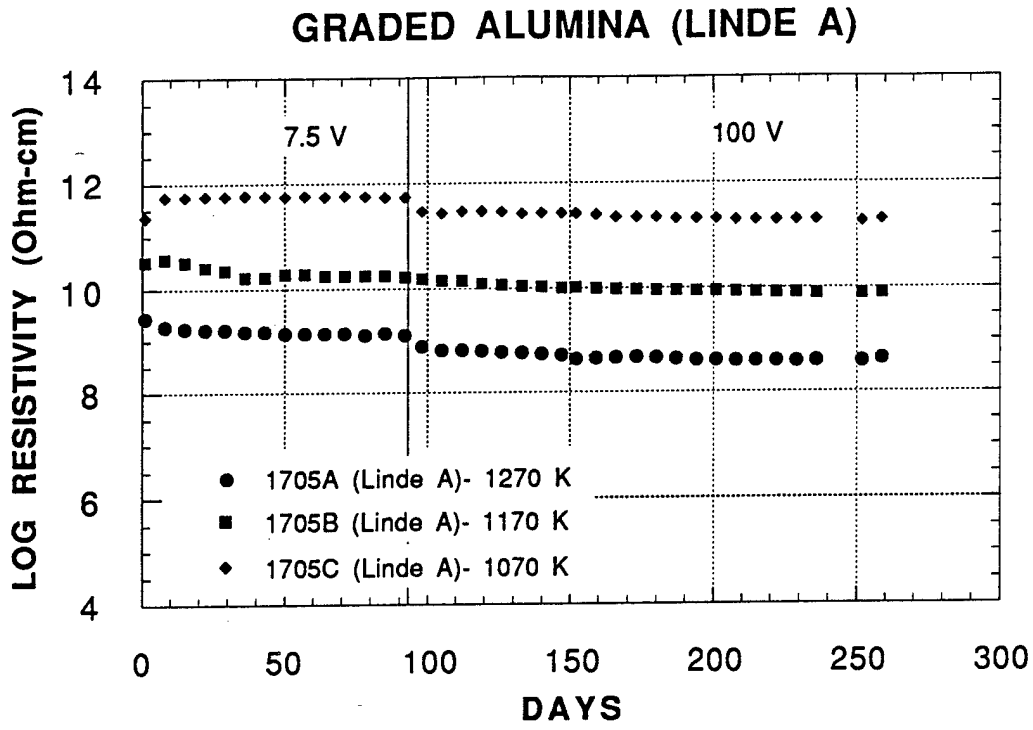

Figure 5-2. Electrical resistivity vs time for GA graded alumina

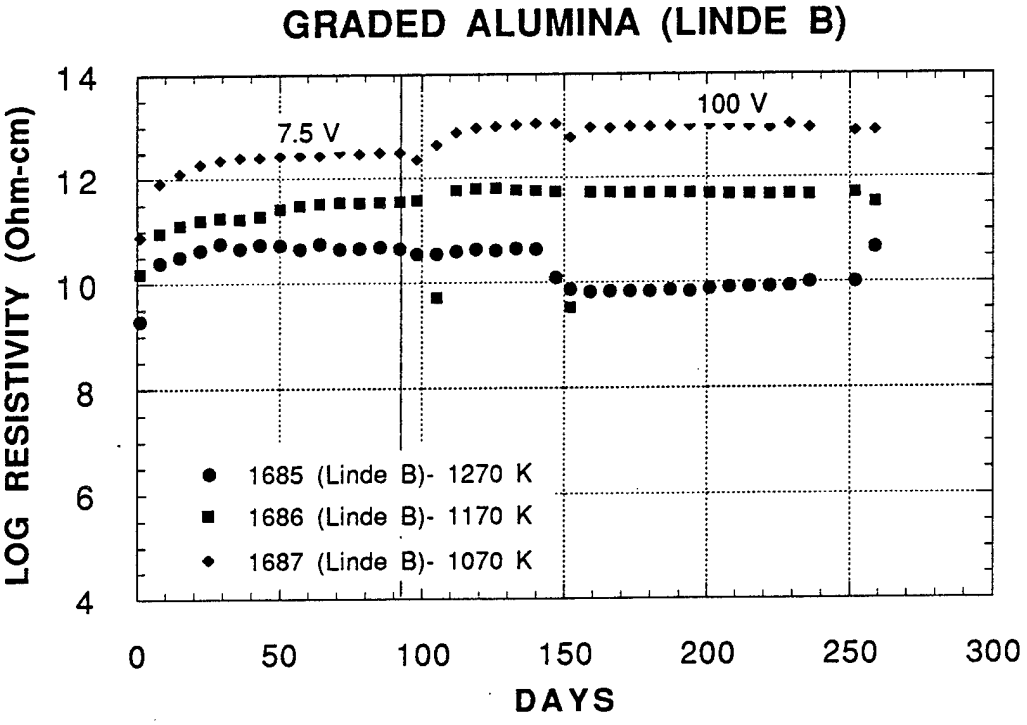

Figure 5-3. Electrical resistivity vs time for GA graded alumina

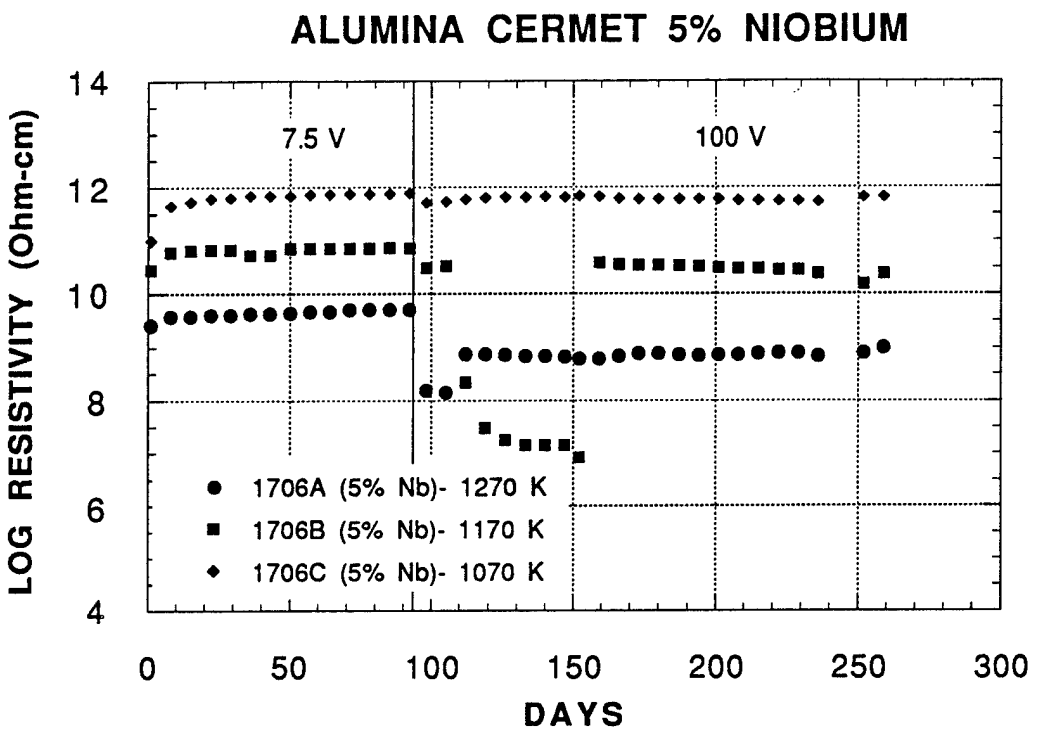

Figure 5-4. Electrical resistivity vs time for TTC alumina cermet (5% Nb)

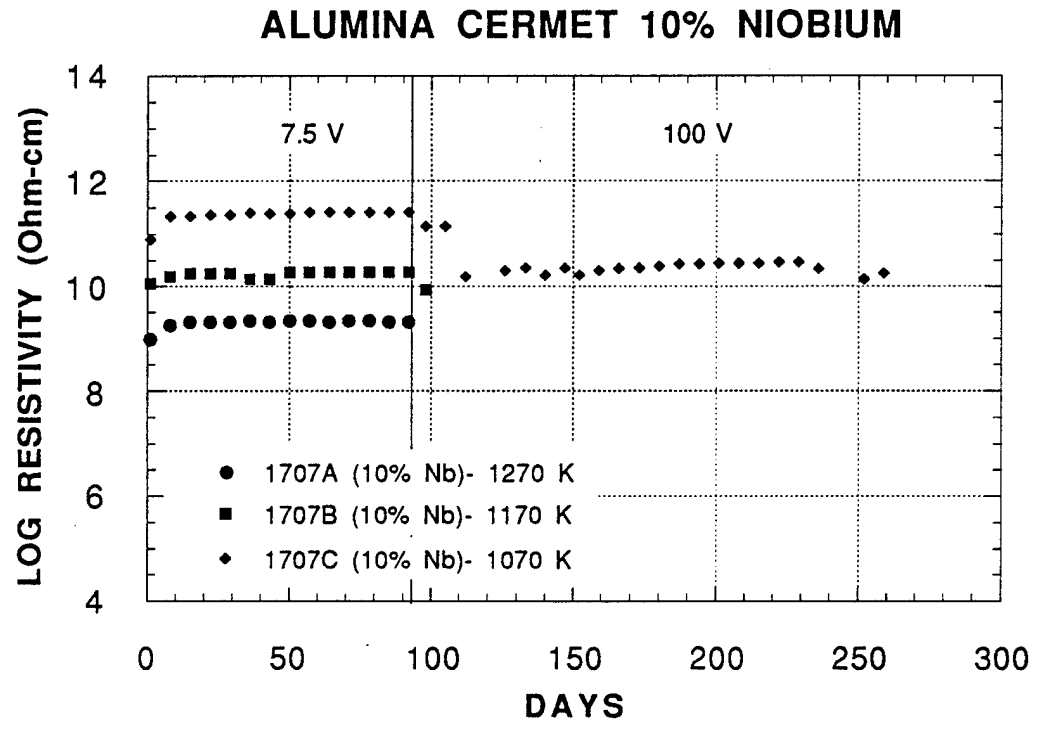

Figure 5-5. Electrical resistivity vs time for TTC alumina cermet (10% Nb)

furnace was turned off several times and all connections inspected to see if there was any reason for this behavior. No discrepancies were found and testing was continued. The performance of the remaining samples as a function of time, temperature, and potential is very good.

5.5 IN-REACTOR TESTING

5.5.1 UCA-3 Irradiation

UCA-3 is the last in the series of in-reactor component testing in EBR-II. It incorporates results from ex-reactor testing as well as results from the postirradiation examination of UCA-1 and UCA-2 sheath insulators. The UCA-3 test consists of two batches of samples, Batch-A and Batch-B. The Batch-B containing the sheath insulator samples was irradiated in cycles 157 and 158, with irradiation ending on January 19, 1992 after having accumulated an estimated peak fast fluence of 1.8×10^{22} n/cm^2 (E>.1 MeV). Disassembly of the capsule and neutron radiography is scheduled for March 1992, and will be shipped to WHC in April for postirradiation examination. Shown on Table 5-1 is the UCA-3 sheath insulator test matrix.

TABLE 5-1

UCA-3 BATCH-B SHEATH INSULATORS TEST MATRIX

Material	Form	Number	End Configuration
Alumina	Graded/Nb	2	Step end
Alumina	Cermet 5% Nb	2	Step end
Alumina	Cermet 10% Nb	2	Step end

5.5.2 IFAC-SI

The IFAC-SI experiment will test sheath insulators in-core with an applied voltage. The test temperature will be the reference operating temperature for SIs, in

the 900 to 1100 K range. It has been shown that SIs have a long life with an applied voltage but no fast neutrons (i.e., ex-reactor testing), and also in a fast neutron environment but without an applied voltage. IFAC-SI will examine SI lifetime with both fast neutrons and an applied voltage.

Work remains on schedule for the delivery of the IFAC-SI test article to WHC in July, 1992. Irradiation in EBR-II is scheduled to begin in May, 1993.

IFAC-SI Test Configuration: As shown in Fig. 5-6, the test articles are two sodium filled heat pipes, the evaporator section of each being made of 3 SIs, electron beam welded end-to-end onto a niobium tube. The SIs are electrically guarded. A screen wick is bonded to the inside of the heat pipe. Once inserted into the reactor, the sheath insulators are heated by gamma heating, and cooled by the evaporator section of the heat pipe. The heat rejection fins are brazed to each heat pipe near the top of its condenser section at two different points so that each will operate at two different temperatures. Since the heat pipe is in a vacuum, most of the heat is rejected by conduction to the walls through the fins, although some heat is also radiated to the canister outer walls, which are cooled by liquid sodium. Inside each heat pipe, the space above the fins is filled with argon buffer gas at a predetermined pressure to maintain the heat pipe temperature. The gas control of the heat pipe works as follows: as each heat pipe evaporator formed by the sheath insulators heats up, the sodium vapor expands, and compresses the argon gas, which then exposes more of the cooling fins, and condenses more sodium vapor, thus cooling the evaporator. The inside of the thimble tube is under vacuum to simulate the environment that the TFE sheath insulator will be exposed to in the space reactor. The complete experiment capsule is shown on Fig. 5-7 and the test configuration within EBR-II is shown schematically on Fig. 5-8.

The test plan calls for one heat pipe (the third one) to be tested in the laboratory while the other two heat pipes are being tested in EBR-II.

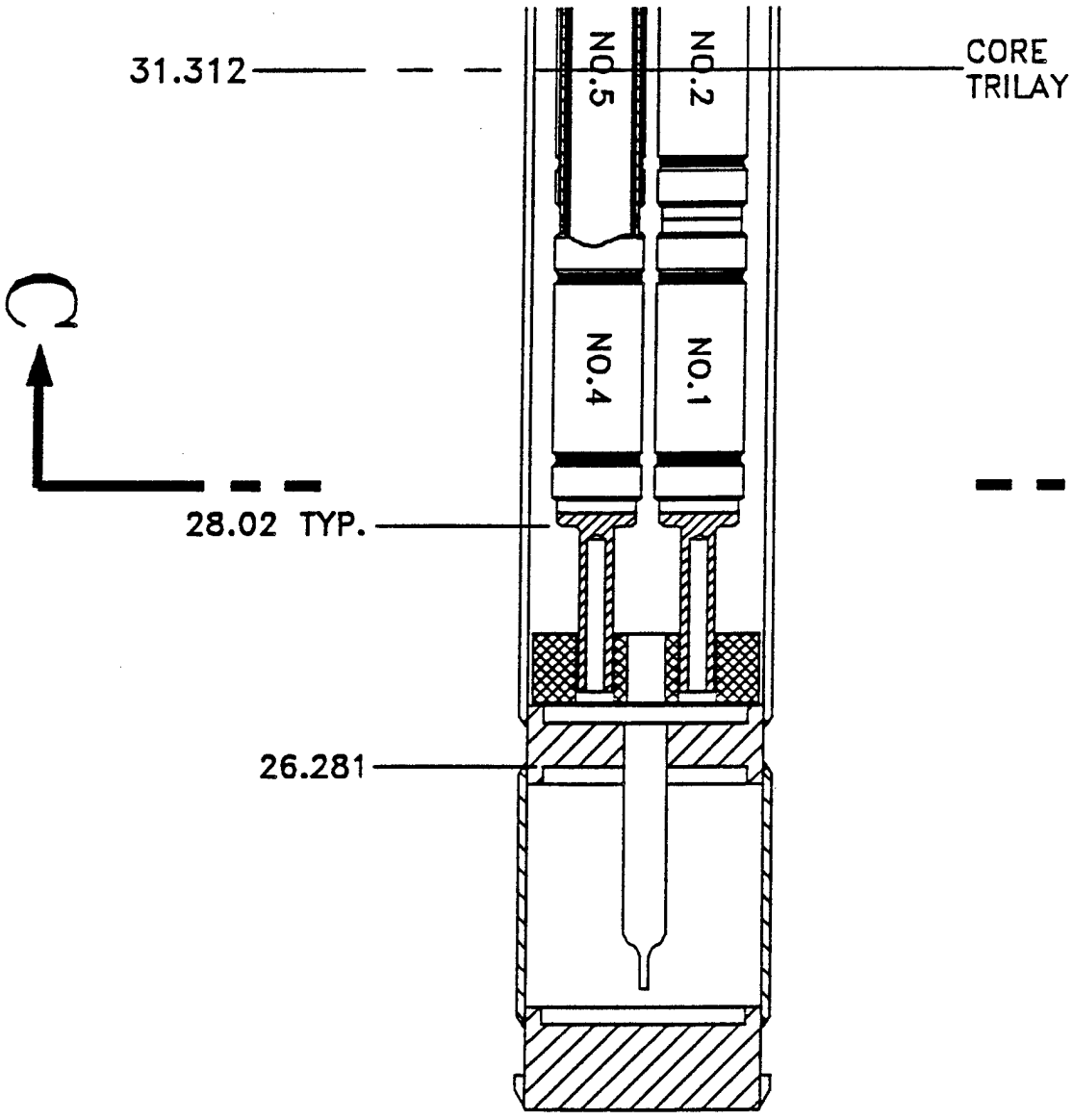

Figure 5-6. Detail of heat pipes in experimental capsule

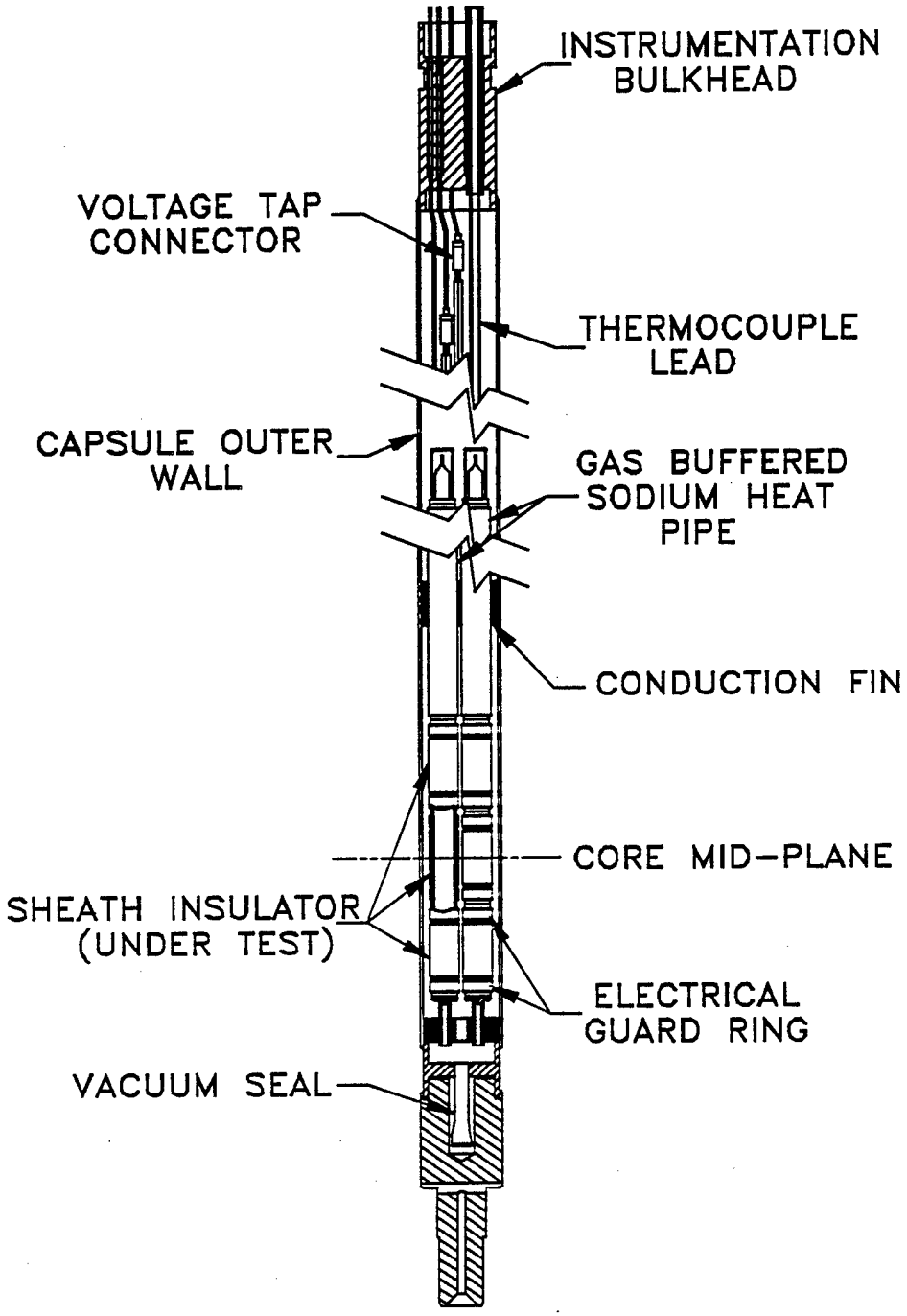

Figure 5-7. Configuration of experiment capsule

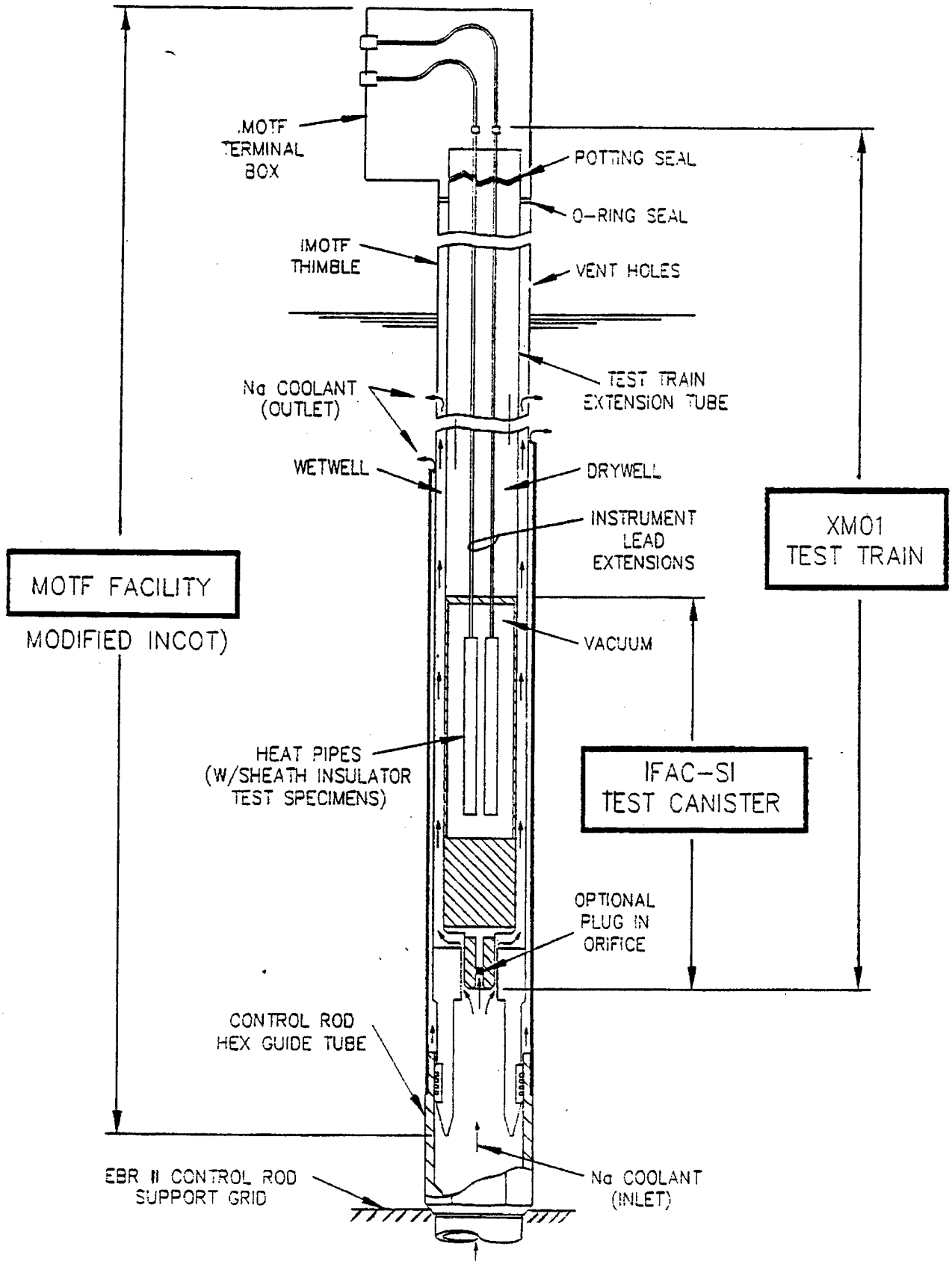

Figure 5-8. IFAC-SI test configuration in EBR-II

Wet Thimble Concept: Over the last 12 months, a decision has been made to use the so-called wet thimble approach in the INCOT facility. As shown on Fig. 5-9, the experimental capsule is enclosed within a steel tube which is inserted into the core inside a hexagonal guide tube.

In the wet thimble approach, sodium will flow in both the hexagonal tube and in the annulus between the experiment and the SS tube. The flow rate of the sodium in the two gaps is set by orifices.

In the original dry thimble approach, a gas gap would have occupied the space between the experimental capsule and the steel tube.

The wet thimble design was selected because it provides adequate cooling of the capsule and it allows the capsule to be removed and reinstalled, or a new capsule to be installed, with minimum of interference of EBR-II operations.

Cooling Fins: With the adoption of the wet thimble design the heat pipe cooling fins were redesigned to increase the cooling capacity. A multiple-slotted design was used to increase the braze contact area while maintaining some flexibility to overcome the mismatch of the thermal expansion between the niobium heat pipe and copper fins. The performance of the slotted fin design was measured in an experiment where the niobium inner tube was heated by electron bombardment and the outer stainless steel tube was water cooled. The results showed that the anticipated heat load of about 1000 W can be rejected by both copper and niobium fins. A sketch of the slotted design is shown on Fig. 5-10.

Fabrication Status: The steady state stress analyses by WHC are complete and transient stress analyses are in progress. The transient thermal analyses of the heat pipes and copper fins were completed. Three dimensional heat transfer analyses are underway to confirm the design.

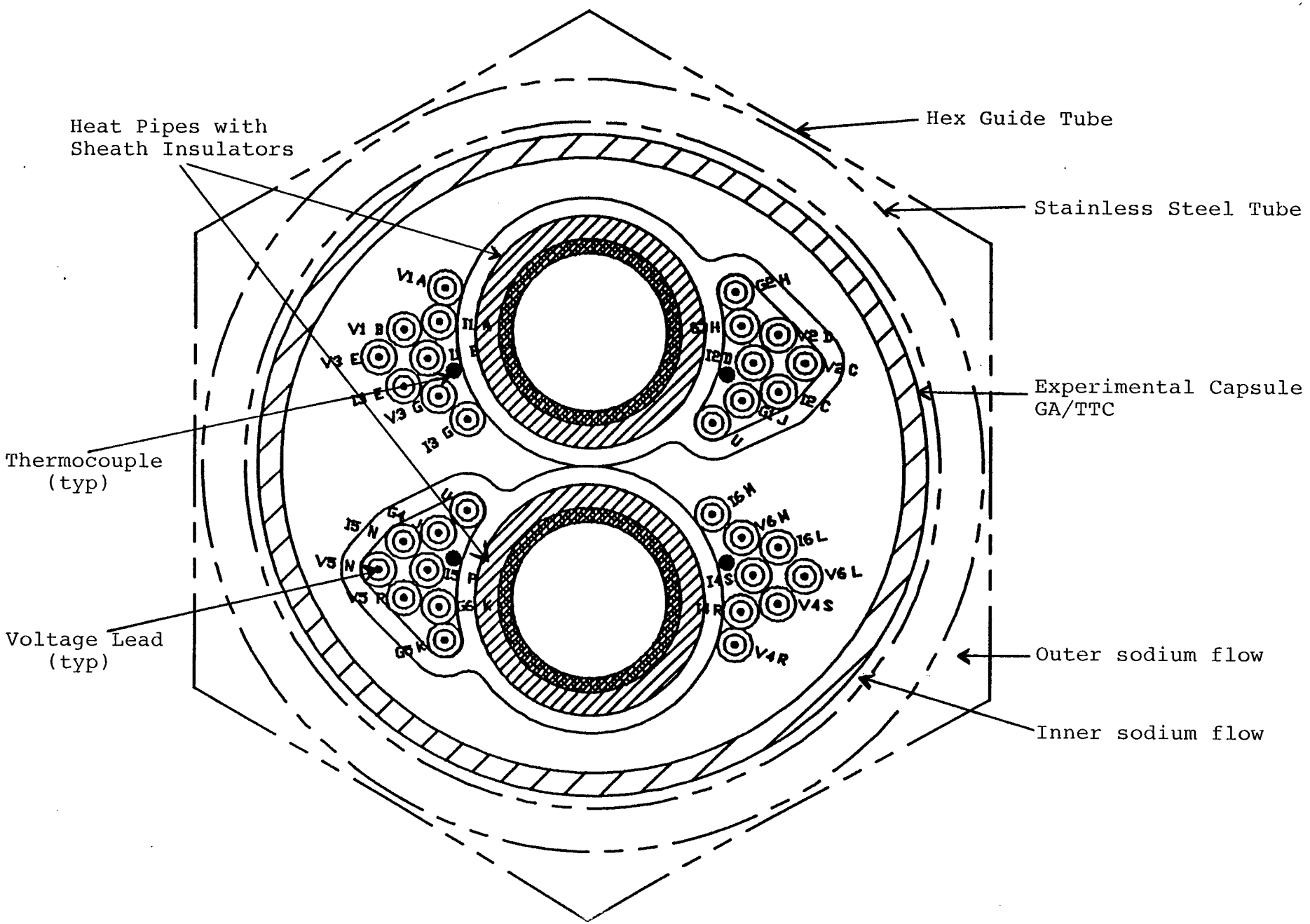

Figure 5-9. Illustration of Wet Thimble Design

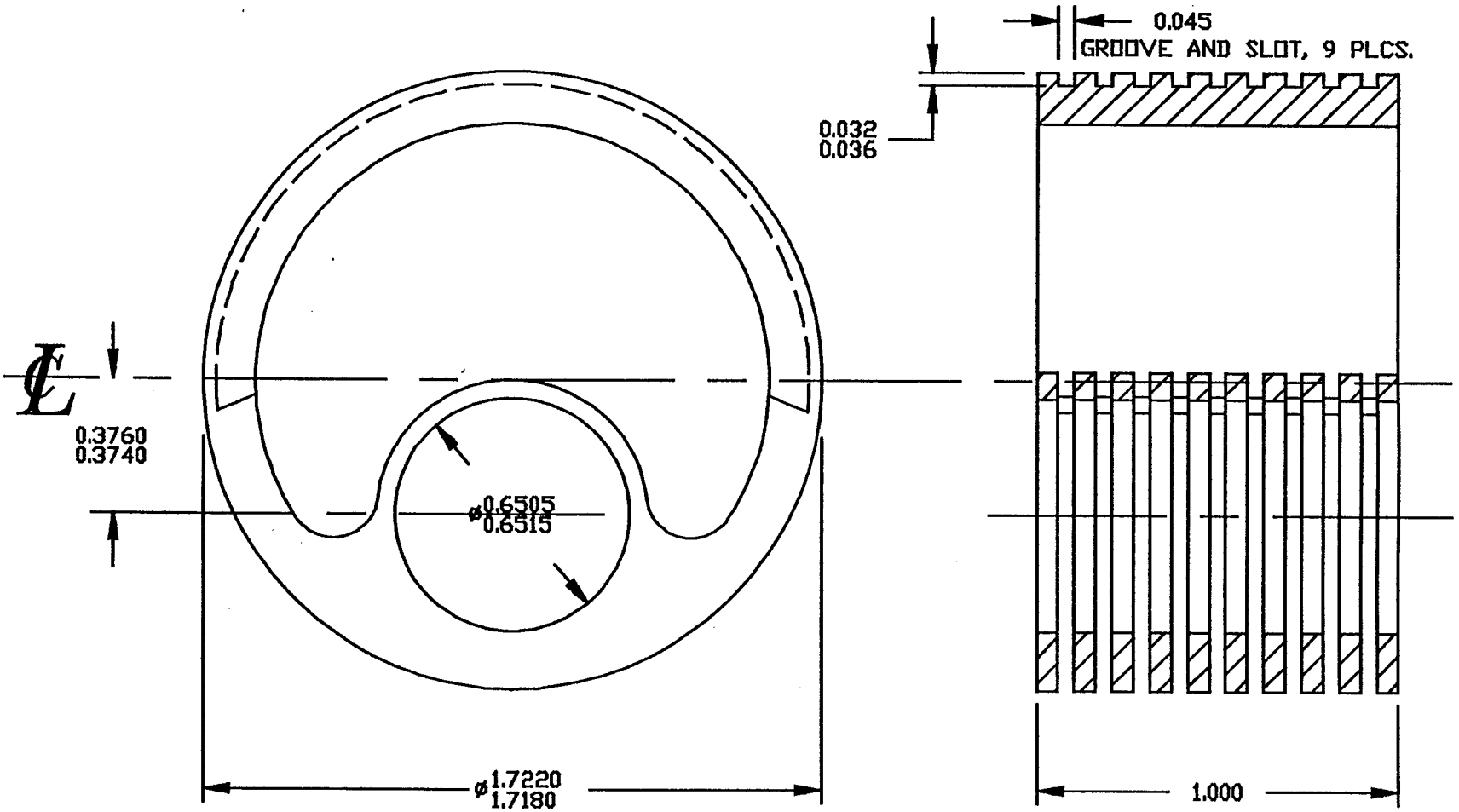

Figure 5-10. Schematic of slotted design of heat pipe cooling fin

Design drawings were completed by WHC with the exception of recent changes requested by ANL to accommodate additional shielding above core and to replace screws in the instrumentation cover tube with a threaded joint.

In-depth testing of the data acquisition system logging and storage functions is nearly complete. The system has performed as designed under the most extreme conditions, storing all data to disk every minute for 4 weeks with no disk changeouts.

The software project management plan and software requirements specification documents are in in final draft form and should be released by the end of March. The verification test plan is also being drafted for the I&C system.

A test bulkhead was fabricated and tested and design modifications are underway. The welds were examined and approved. The electrical test was successful. A picture of the test assembly is shown in Fig. 5-11.

Trilayer sheath insulators are on hand for 3 heat pipes. The heat pipe component fabrication is completed, awaiting the fabrication of the screen wick at LANL. As soon as that is received the assembly will continue. The argon fill pressure will be adjusted during heat pipe processing and charging to achieve the proper operating temperature. One heat pipe will be put on electrical test in an ion pumped system. The test bell jar has been completed and is shown in Fig. 5-12.

Wick Options: Obtaining wicks for the heat pipes is a long lead-time effort. Options considered were:

1) Procure high purity Nb mesh.
2) Produce a Mo screen wick.

The Nb mesh can be bonded with Ni but obtaining mesh of the right size and purity in a timely manner was very difficult.

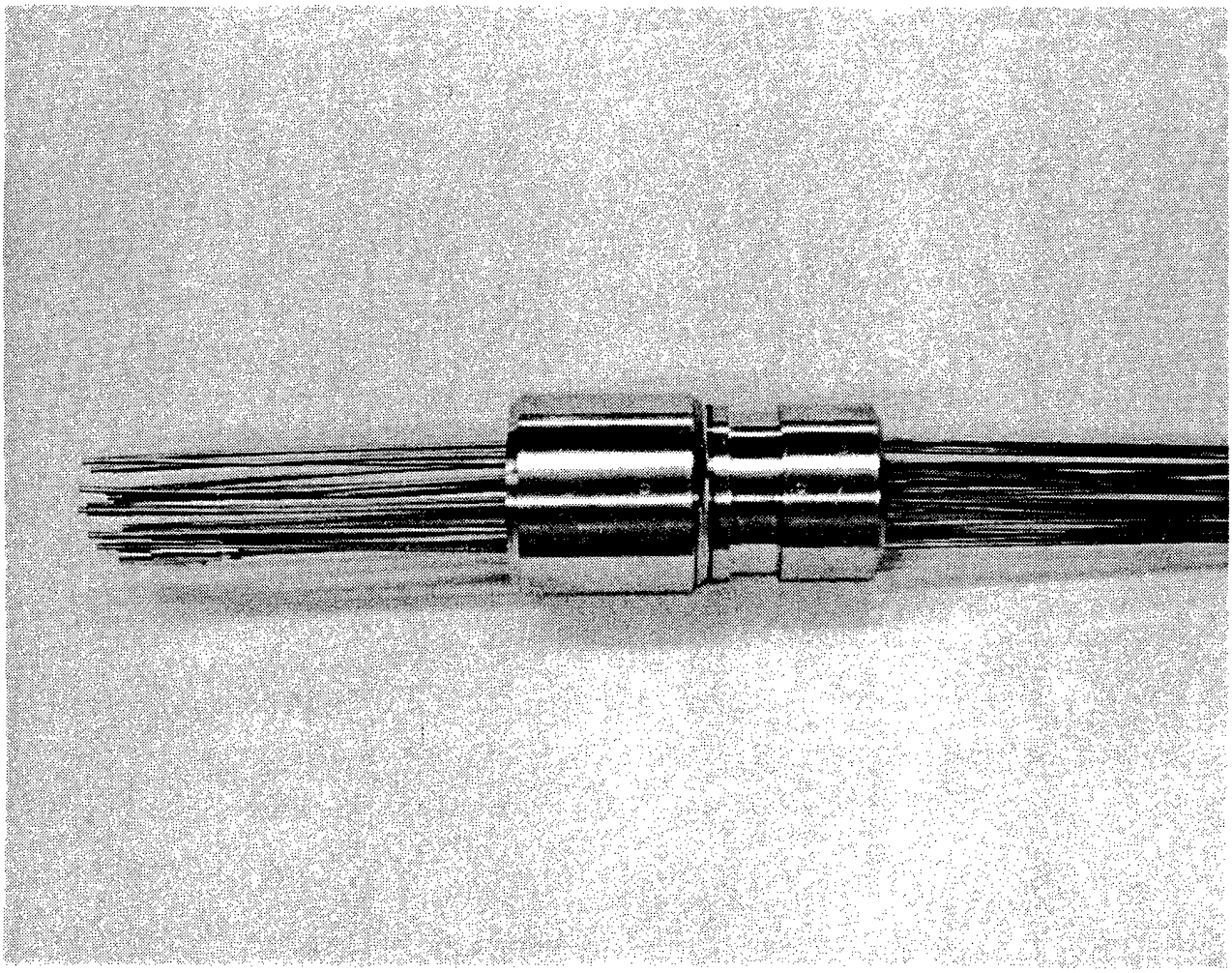

Figure 5-11. IFAC-SI Bulkhead Assembly

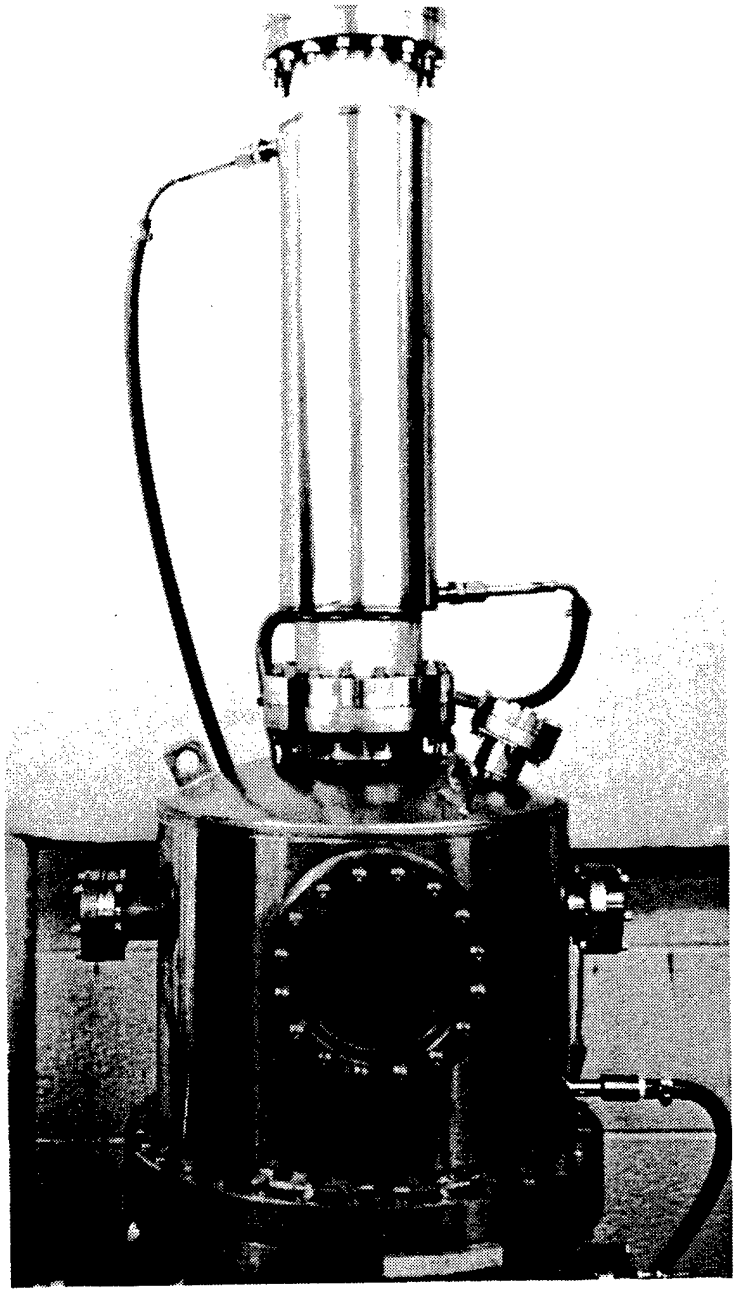

Figure 5-12. IFAC-SI Test Bell Jar

The Mo screen was on hand but not yet certified. Bonding of the screen to the inner wall appeared to be a potential problem so a decision was made to obtain a free-standing Mo screen wick from LANL. The fabrication process would also assure the required wisk purity.

Electrically Tested Heat Pipe Results: Two electrical tests were performed at Thermo Electron Technologies. In the first experiment, the sheath insulators were heated by radio frequency (RF) induction, and in the second experiment by radiation in a Multi-Foil furnace. The heat pipe was first tested for heat transfer capacity and temperature uniformity by RF induction heating at three settings of RF power. The temperature of the heat pipe was measured with an optical pyrometer sighting on the grooved surface. The test temperatures were 1033 K, 1078 K, and 1118 K. In this experiment the heat output was calculated based on the heat rejected by radiation. Assuming that the emissivity of the grooved section was 0.5, and that the sheath insulators had an emissivity of 0.2, then the heat radiated from the whole pipe varied from about 1100 W to 1530 W. This value is above the 1000 W heat transfer that would be expected during the reactor tests. The temperature uniformity was also measured and the heat pipe was essentially isothermal within 5 K. This experiment proved that the basic design was adequate.

In the second experiment, a Multi-Foil furnace (Ref. 5-1) was first operated at the test temperature without the heat pipe in order to measure the standby losses. Next, 25% of the heat pipe was inserted, and the furnace was heated until the temperature of 1120 K was reached. At this temperature the net power input to the furnace (power input less standby losses) was 1233 W. To compare these results with the RF tests, where the entire heat pipe was radiating, the power must be reduced by 25%. The results from the two experiments agree within 7 percent.

These experiments show that a heat pipe can successfully be assembled by electron-beam welding sheath insulators end-to-end, and connecting them onto a

niobium tube equipped with a screen wick. The heat transferred by the test heat pipe was up to 1500 W, which was judged adequate for dissipating the expected gamma heating in the reactor experiment. The temperature of the test heat pipe was uniform to 5 K.

Sheath Insulator Test Specimens: The graded alumina and alumina cermet with 5 and 10% niobium sheath insulators selected for the IFAC-SI test have been electrically tested at 1300 K for several days. All the samples showed resistivity values greater than 10^8 ohms-cm at temperature.

The current graded samples for IFAC-SI were fabricated in early 1990. The alumina used on these samples was a sol-gel derived material. Currently the type of alumina we are testing is commercial alumina of similar purity to the sol-gel alumina. A change was made to go back to the commercial alumina due to the high costs of making alumina, especially when the electrical properties for both kinds of materials are very similar. The sol-gel material was tested out-of-core by RAI at real time and accelerated conditions as FY-90 samples. The commercial alumina is being tested at RAI at real time and accelerated conditions as FY-91 samples. There is very little difference in the electrical behavior of both materials. Both types of alumina are acceptable as sheath insulator material.

5.3.3 Thermal Conductivity of Irradiated Sheath Insulators

In addition to having good electrical resistance, sheath insulators must have good thermal conductivity at the TFE operating conditions. The objective of this Air Force funded task was to measure the thermal conductivity of irradiated sheath insulator samples. The work was done by WHC.

A new measuring system was procured which uses a pulse technique generated by a flash lamp that can deliver up to 3000 watts of energy. The system was

installed and successfully tested. Laboratory measurements of thermal diffusivity were successfully completed on nine unirradiated sheath insulators as shown in Table 5-2. The samples included three graded alumina, three alumina cermet with 10% niobium, two alumina cermet with 5% niobium and a graded yttria sheath insulator. A niobium cylinder of the same geometry as the unirradiated sheath insulator sample was used as a control sample.

The measured thermal conductivity of the control sample agrees within $\pm$1% of the published value for niobium. A data base is now available for comparison to irradiated specimens. The requirement for SI is a thermal conductivity greater than .03 W/cm-K.

TABLE 5-2

MEASURED THERMAL CONDUCTIVITY OF SHEATH INSULATORS

1173 K		973 K	
Specimen	Thermal Conductivity (W/cm-K)	Specimen	Thermal Conductivity (W/cm-K)
Niobium	0.677	Niobium	0.703
10% Nb Cermet (067-6)	0.292		
10% Nb Cermet (065-3)	0.249	10% Nb Cermet (065-3)	0.280
10% Nb Cermet (No ID)	0.209	10% Nb Cermet (No ID)	0.248
5% Nb Cermet (066-1)	0.254	5% Nb Cermet (066-1)	0.242
5% Nb Cermet (068-3)	0.244	5% Nb Cermet (068-3)	0.282
Graded (031069-3)	0.180	Graded 031069-3	0.211
Graded (No ID)	0.171	Graded (No ID)	0.192
Graded (Short)	0.170		
Graded Yttria (Y-4)	0.100	Graded Yttria (Y-4)	0.120

TRIGA Testing: The desirability of doing IFAC-SI tests in TRIGA has also been studied. From the cost and assessability point of view, TRIGA is excellent. However, the fast neutron fluence is small and only real time testing is possible.

5.6 STATUS SUMMARY

A summary of the sheath insulator development effort is shown in Table 5-3. The development priority at the moment is as follows:

Reference material:	Aluminum oxide
Design:	Trilayer
Fabrication:	Plasma sprayed graded or slip cast cermet.

Polycrystalline aluminum oxide both graded and cermet has shown good ex-reactor and in-reactor electrical properties. It has survived fast neutron fluences 2-1/2 times higher than what is expected in a seven year lifetime. Polycrystalline aluminum oxide plasma sprayed graded trilayer has experienced over 30,000 real time test hours in the TRIGA reactor.

References

5-1 TFE Verification Program Semiannual Report for the Period Ending September 30, 1991, GA-A20804.

Table 5-3
SHEATH INSULATOR TECHNOLOGY STATUS

Material	Priority	Electrical Properties	Neutron Stability	Fabricability	Test Matrix (No. of Specimens)					
					UCA-1	UCA-2	UCA-3	TFE 1H1, 1H2, 1H3, 3H1 3H5, 6H1	Fueled Emitter	Ex-Reactor
Y_2O_3 (PC)	Low	Poor	Good	Good	3	4		1		23
YAG (PC)	Low	Good	Good	Difficult*	3	2				7
Al_2O_3 (PC)	High	Good	Good	Good	10	4	6	12	9	34
Al_2O_3 (SC)	Low	Good	Acceptable	Difficult						2

PC Polycrystalline.
SC Single Crystal

6. FUELED EMITTER TASK

6.1 OBJECTIVE AND TECHNICAL APPROACH

The function of the fueled emitter is to generate the heat necessary to drive the thermionic conversion process with the geometry, power densities and temperatures required by the reference TFE design, using materials compatible with both the thermionic process and reactor requirements. Specific requirements for the emitter are given in Table 6-1.

TABLE 6-1

FUELED EMITTER DESIGN REQUIREMENTS

Emitter	
Material	Duplex tungsten
Outside diameter, cm	1.27
Thickness, cm	0.10
Emitter/collector gap, cm	0.025
Nominal temperature, K	1800
Fuel	
Outside diameter, cm	1.0
Inside diameter, cm	Variable
Enrichment, % U-235	93
Fuel length, cm	4.65
Nominal fuel burnup, atom percent	4.1
Peak fuel burnup, atom percent	5.3

The key technical concern is the emitter distortion as a result of fuel swelling over the 7-year lifetime. It is the objective of the fueled emitter task to develop and demonstration by appropriate ex-reactor testing, in-reactor testing and analytical verification a fueled emitter capable of meeting the above design requirements.

The strategy to demonstrate the performance and lifetime of the fueled emitter is based on extensive in-reactor testing. While duplex tungsten will be the focus of most of the testing, alternate materials, particularly the HfC strengthened materials, look very promising and will be considered. Additionally, alternate fuel forms will be evaluated which either weaken the fuel or change its swelling characteristics, thereby minimizing emitter distortion. These forms include insulated fuel, and wafered fuel.

The uninstrumented fast reactor accelerated component (UFAC) test program in EBR-II consists of three batches of fueled emitters (FEs). The accelerated testing of several specimens in Batch 1 has been completed and the PIE is underway. The accelerated specimens in Batch 2 completed their irradiation in January, 1992, and PIE will begin in the near future. The real time specimens of Batch 1 and Batch 2 are currently under irradiation. Batch 3 is planned for FY-93.

A road map showing the irradiation strategy for the FEs in EBR-II is shown on Fig. 6-1. More detail is shown on Table 6-2 which also shows the current irradiation status of the test vehicles. The recent irradiation history and the FY-92 projection are shown on Fig. 6-2 for both the UFAC subassemblies and EBR-II. Periodically, an interim nondestructive examination is performed during which a neutron radiography (NR) is taken, and at that time the letter designation of the subassembly is changed, e.g., UFAC-1 to UFAC-1A, etc.

The FE identification scheme is shown on Table 6-3 for Batches 1 and 2. A summary of the status of each FE is shown on Table 6-4.

6.2 EMITTER THINNING

Emitter thinning as a result of irradiation was first observed in TFE-1H1. A schematic picture of the observation is shown on Fig. 6-3. The greatest effect was near the W/Re fuel pedestal, or heat shield used to protect the bottom of the emitter.

Figure 6-1

ROAD MAP: FUELED EMITTER TESTING IN EBR-II

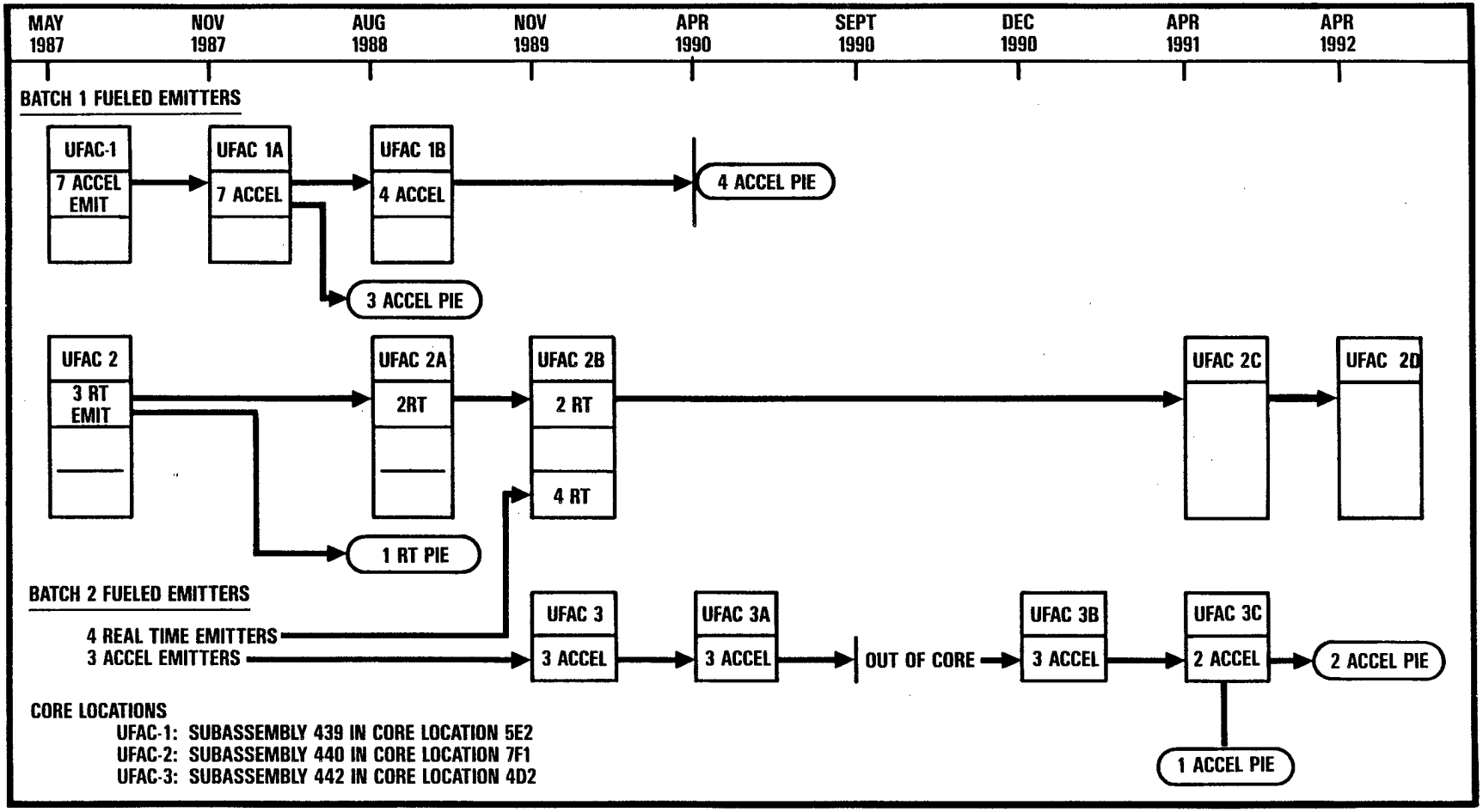

TABLE 6-2
SUMMARY STATUS OF UFAC TEST SERIES IN EBR-II AS OF MARCH 1, 1992

Test Designation	Test Content	Status	EFPD*	Irradiation Fast Fluence $x10^{22}n/cm^2$	Peak Burnup (at.%)	Postirradiation Examination Status*
UFAC-1	7 Batch-1 FEs	Complete 8-87	94.5	1.5	1.0	NDE 7 capsules complete 11-87
UFAC-1A	7 Batch-1 FEs	Complete 4-88	221.5	3.6	2.1	NDE 7 capsules complete 7-88 DE 3 capsules complete 6-89
UFAC-1B	4 Batch-1 FEs	Complete 4-90	518	7.6	4.3	NDE 4 capsules complete 6-90
UFAC-2	3 Batch-1 FEs	Complete 4-88	285	2.8	0.5	NDE 3 capsules complete 6-88 DE 1 capsules complete 6-89
UFAC-2A	2 Batch-1 FEs	Complete 3-89	467	4.2	1.1	NDE 2 capsules complete 6-89
UFAC-2B	2 Batch-1 FEs 4 Batch-2 FEs	Complete 4-91	798 331	7.5 2.9	2.0 .85	NDE 6 capsules complete
UFAC-2C	2 Batch-1 FEs 4 Batch-2 FEs	Complete 1-92	908 441	8.5 4.1	2.3 1.1	NDE 6 capsules in progress
UFAC-2D	2 Batch-1 FEs 4 Batch-2 FEs	Begin irrad 5-92	0	0	0	
UFAC-3	3 Batch-2 FEs	Complete 4-90	64	1.1	0.66	NDE 3 capsules complete 5-89
UFAC-3A	3 Batch-2 FEs	Complete 9-90	172	2.9	1.73	NDE 3 capsules complete 11-90
UFAC-3B	3 Batch-2 FEs	Complete 4-91	266	4.5	2.7	NDE 3 capsules complete
UFAC-3C	2 Batch-2 FEs	Complete 1-92	376	6.2	3.5	NDE 5 capsules in progress

* Equivalent full power days.

* NDE: nondestructive examinations: visual, dimensional, gamma-scan, neutron radiography.

* DE: destructive examinations: gas sampling, radiochemical burnup, metallography.

FIGURE 6-2

UFAC IRRADIATION SCHEDULE

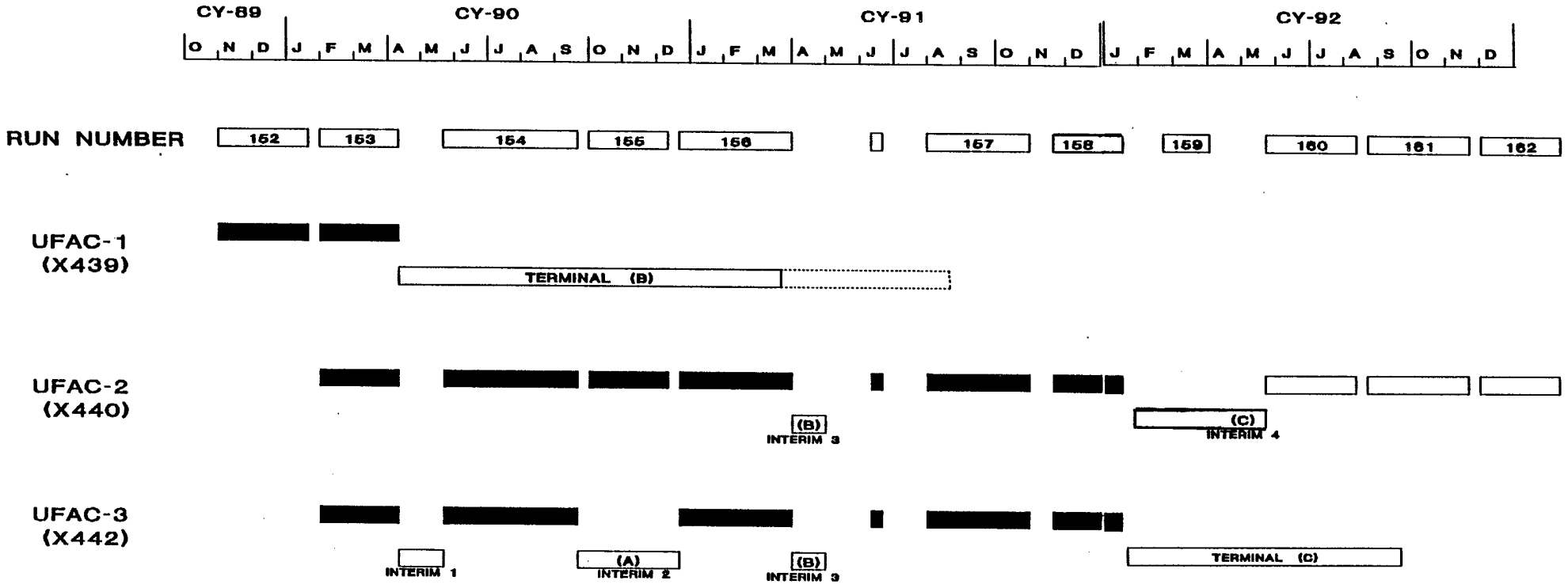

TABLE 6-3

UFAC EMITTER IDENTIFICATION SCHEME

ID Number Real Time	ID Number Accelerated	Diameter	Thickness	Temperature	Fuel Design	Comments
				UFAC BATCH-1		
SU2-1		0.5	0.040	1800	15% void	Reference design
SU2-2		0.5	0.050	1800	15% void	Thick emitter
SU2-3*		0.5	0.040	1800	Solid	Solid fuel
	SU1-4	0.25	0.020	1700	15% void	Reference design/low temperature
	SU1-5	0.25	0.020	1800	15% void	Reference design
	SU1-6*	0.25	0.020	1900	15% void	Reference design/high temperature
	SU1-7*	0.25	0.020	1800	Solid	Solid fuel
	SU1-8	0.25	0.020	1900	Solid	Solid fuel/high temperature
	SU1-9	0.25	0.025	1800	15% void	Thick emitter
	SU1-10*	0.25	0.025	1900	15% void	Thick emitter/high temperature
				UFAC BATCH-2		
SU2-11		0.5	0.040	1800	15% void	Batch-1 replica
SU2-12		0.5	0.040	1800	15% void	High fuel void
SU2-14		0.5	0.040	1800	-	Insulated fuel
SU2-15		0.5	0.040	1800	-	Wafered fuel
	SU3-16	0.25	0.020	1800	15% void	Batch-1 replica
	SU3-17	0.25	0.020	1800	-	Insulated fuel
	SU3-20	0.25	0.020	1800	-	Wafered fuel

*Removed for examination at end of Run 147.

TABLE 6-4
STATUS OF UFAC FUELED EMITTERS (MARCH 1, 1992)

ID Number Real Time	ID Number Accelerated	Test Status	Last EBR-II Run	Burnup (a/o)	Fluence (10^{22}nvt)	Reason for Removal or Condition Upon PIE
Batch 1						
SU2-1		In-core	N/A	2.0	7.6	N/A
SU2-2		In-core	N/A	2.3	8.5	N/A
SU2-3		Removed for PIE	147	.45	2.8	Fractured emitter
	SU1-4	End of test	153	3.8	7.1	Fractured @ w/Ta transaction
	SU1-5	End of test	153	3.8	7.2	Breached
	SU1-6	Removed for PIE	147	1.7	3.2	Fractured emitter
	SU1-7	Removed for PIE	147	1.4	2.9	Fractured emitter
	SU1-8	End of test	153	3.2	6.8	Intact
	SU1-9	End of test	153	4.3	7.6	Intact
	SU1-10	Removed for PIE	147	1.9	3.3	Fractured emitter
Batch 2						
SU2-11		In-core	N/A	.96	3.7	N/A
SU2-12		In-core	N/A	1.0	4.1	N/A
SU2-14		In-core	N/A	.96	3.7	N/A
SU2-15		In-core	N/A	1.1	3.2	N/A
	SU3-16	Removed for PIE	158	2.8	5.9	Intact
	SU3-17	Removed for PIE	156	2.7	4.5	Excessive emitter deformation and fuel redeposition
	SU3-20	Removed for PIE	158	3.5	6.2	Intact

It was postulated that a chemical reaction involving the Re could occur that resulted in the creation of a corrosive liquid that could cause erosion of the W emitter. Reaction with fission products was also considered possible. A complete survey of all emitters was then made to correlate emitter thinning with test article materials and irradiation parameters.

6.2.1 Chemical Reactions Considered

At the high irradiation temperatures (1800-2600 K), the UO_2 will dissociate and liberate various vapor species, e.g., U(g), UO(g), UO_2(g). The relative partial pressures of U(g), UO(g), UO_2(g) will be fixed by the temperature. During vaporization UO_{2+x} will preferentially lose oxygen until a congruently vaporizing composition is obtained. At this composition the U activity may be sufficiently high to allow reaction with Re in the fuel pedestal and top disc to form URe_2. At irradiation temperatures the URe_2 will be liquid and quite mobile. Liquid URe_2 and liquid U-intermetallics in general, have the potential to corrode and thin the W emitter wall.

There are many possible chemical reactions involving Re, U, O_2 and fission products. Three examples are:

(1) $UO_2 + Re \rightarrow ReO_2 + U$

(2) $2UO_2 + 4Re \rightarrow URe_2 + 2ReO_2 + U$

(3) $UO_2 + 3Re \rightarrow URe_2 + ReO_2$

Uranium is a liquid about 1400 K, and ReO_2 is a liquid above 1475 K. Reaction (3) is exothermic, and reaction (2) can be exothermic depending on fuel stoichiometry, as shown in Fig. 6-4. The solid lines in Fig. 6-4 are for $UO_{2.002}$ and the dashed lines are for $UO_{2.006}$. There are many other reactions that could be involved but the ones shown indicate a potential for Re catalyzed chemical attack.

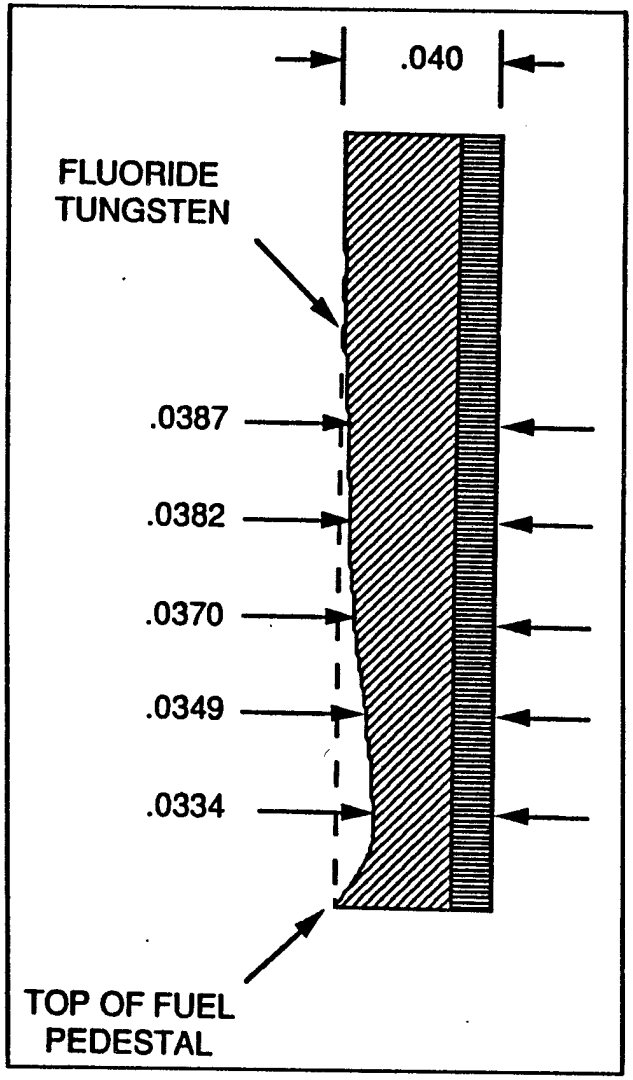

Figure 6-3. Emitter Thinning in TFE-1H1

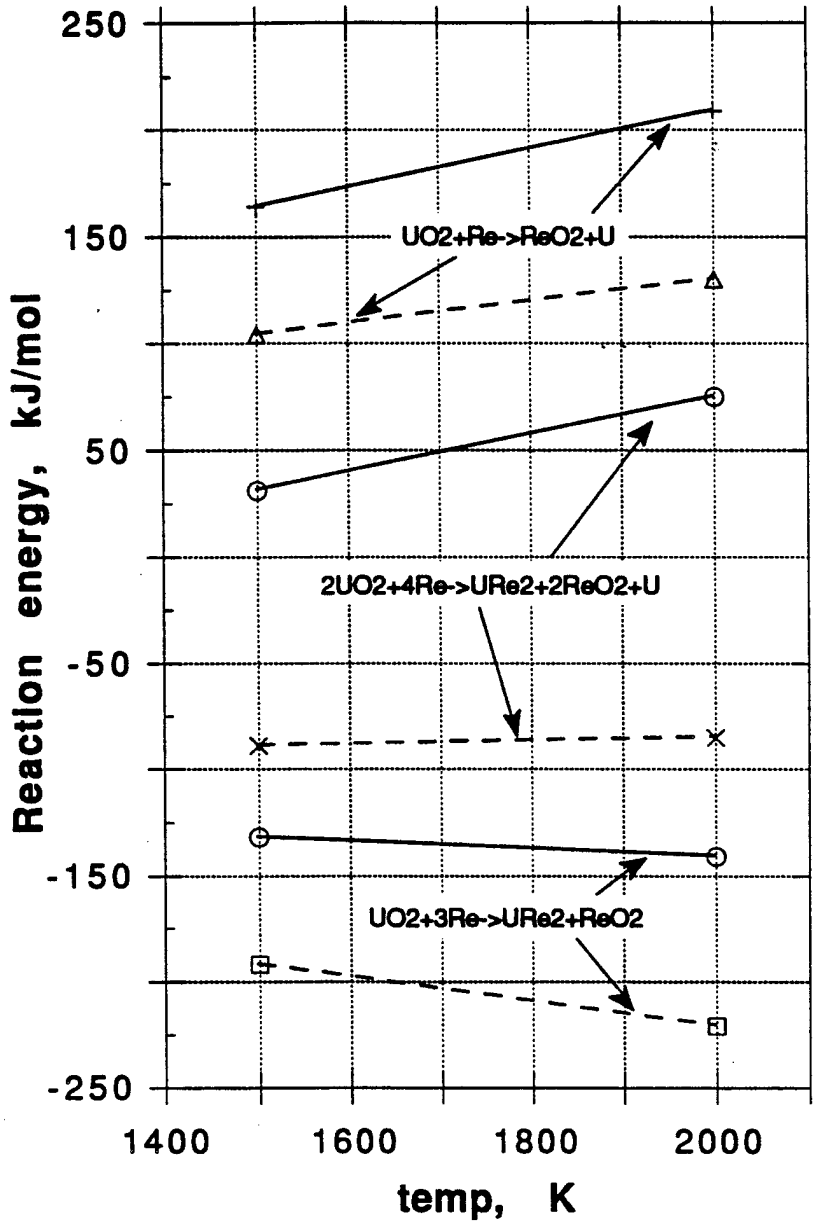

Figure 6-4. Reaction Energy vs Temperature

6.2.2 Emitter Thinning in Test Articles

To quantify emitter thinning, the axial dependence of emitter thickness was measured for several emitters, the measurements being defined as shown in Fig. 6-5. The results are shown in Table 6-5.

TABLE 6-5

EMITTER THINNING DATA: CHANGE IN EMITTER THICKNESS (Mils)

TEST ARTICLE	BURNUP a/o	DISTANCE FROM PEDESTAL TOP					
		0 in	.05 in	.10 in	.15 in	.20 in	.25 in
TFE-1H1	-	0	7	5	3	2	1
TFE-1H3	-	3	5	2	0	0	0
SU2-1	1.9	0	0	1	1	0	0
SU2-2	2.1	0	0	0	0	1	1
SU1-4	3.8	5	3	0	0	0	0
SU1-5	3.8	4	6	4	1	1	2
SU1-8	3.2	1	4	1	0	0	0
SU1-9	4.3	3	1	0	0	0	0
SU3-16	1.9	0	0	0	0	0	0
SU3-20	1.9	0	0	<1	<1	0	0
SP-100 Capsule 2							
2.1		1	0	0	0	0	0
2.2		0	3	0	0	0	0
2.3		0	0	0	0	0	0

These data are summarized on Table 6-6 for those emitters that had a W/Re pedestal and on Table 6-7 for those emitters that had a W pedestal. The correlation between emitter thinning and the presence of Re in the pedestal is very strong.

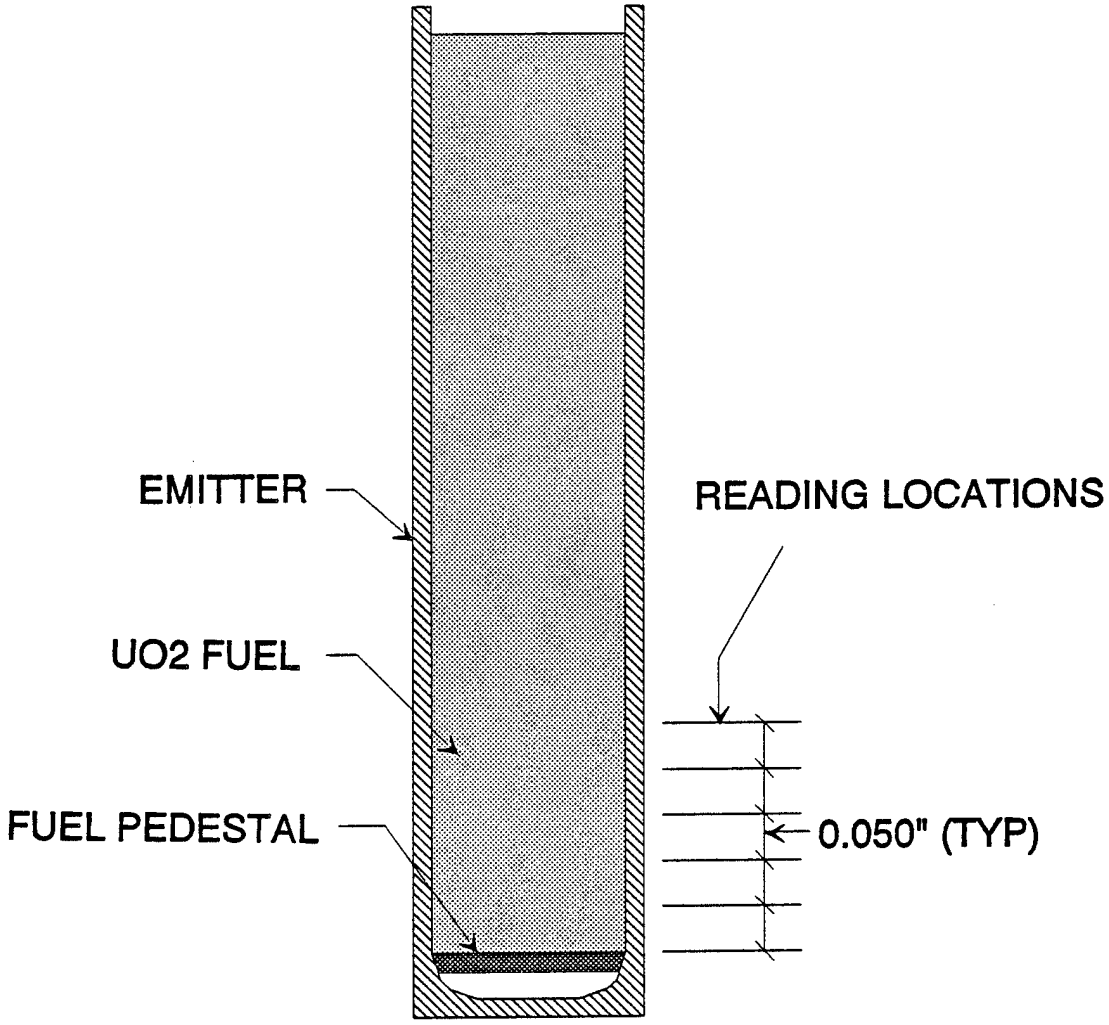

Figure 6-5. Fueled Emitters Wall Thickness Readings

TABLE 6-6

EMITTER WALL THICKNESS CHANGE: EMITTERS WITH W/Re FUEL PEDESTALS

Type	Designation	Burnup (at %)	Irradiation Time (Hours)	Wall Thickness (mils)
TFE	1H1	1.33	13,959	7
	1H3	.65	7,217	5
	1H2	.27	2,828	0
	3H1		4,255	Yes
Batch 1, Accel	SU1-4	3.8	12,449	5
	SU1-5	3.8	12,449	6
	SU1-8	3.2	12,449	4
	SU1-9	4.3	12,449	3
Batch 1, Real	SU2-1	1.9	18,912	1
	SU2-2	1.9	18,912	1

TABLE 6-7

EMITTER WALL THICKNESS CHANGE: EMITTERS WITH W-ONLY FUEL PEDESTALS

Type	Designation	Burnup (at %)	Irradiation Time (Hours)	Wall Thickness (mils)
Batch 2, Accel	SU3-16	1.9	8,760	<1
	SU3-20	1.9	8,760	<1
Batch 2, Real	SU2-11	.76	7,728	0
	SU2-12	.76	7,728	0
	SU2-14	.76	7,728	0
	SU2-15	.76	7,728	0
SP-100	2.1	.51	38,982	1
	2.2	.92	38,982	3
	2.3	.75	38,982	0

This conclusion is reinforced by the microprobe analysis of the SU1-4 emitter that was performed during PIE at WHC. This is discussed more fully in Section 6.4.1.

6.3 EMITTER DEFORMATION: REAL TIME EMITTERS

As outlined on Table 6-4, 2 Batch-1 and 4 Batch-2 real time fueled emitters continue irradiation in UFAC-2. Emitter deformation was measured after .76 a/o burnup with the results shown on Table 6-8. With the exception of SU2-14, which contains "insulated" fuel, the deformations are not significant. However, for the test specimen that contains a thin layer of depleted UO_2 around the core of enriched UO_2, the deformation is significant. The function of the depleted UO_2 layer is to raise the temperature of the enriched UO_2 so it can more easily deform to accommodate fission product induced swelling. Further testing of the insulated fuel concept is not planned and SU2-14 will be removed from UFAC-2.

The wafered fuel concept has the least swelling. It contains W disks to enhance heat transfer to the emitter to reduce the average UO_2 temperature.

TABLE 6-8

EMITTER DEFORMATION - REAL TIME EMITTERS

Emitter ID	Burnup a/o	Deformation	
		mils	%
SU2-1	1.90	6.4	2.6
SU2-2	1.90	5.3	2.1
SU2-11	.76	0.9	.7
SU2-12	.76	1.2	1.0
SU2-14	.76	5.5	4.5
SU2-15	.76	nil	nil

6.4 UFAC-1 FUEL EMITTER STATUS

6.4.1 UFAC-1B Metallography

A metallographic examination of the accelerated emitters from Batch-1 was completed in late FY-91 by Westinghouse Hanford Company under a contract from the Air Force Phillips Laboratory. The results of this work are presented in Ref. 6-1.* A brief summary of the metallographic examination derived from Ref. 6-1 is presented here.

The extent of the metallography is shown in Table 6-9 and on Fig. 6-6. Seven samples were studied: 3 from SU1-4, 2 from SU1-5, 1 from SU1-8 and 1 from SU1-9.

Generally, examinations showed fuel structures consistent with expected temperatures and previous examinations. Extensive reactions occurred in the area of the lower W-26 Re heat shields and to a lesser extent in the area of the upper heat shields. Similar interactions in the area of the heat shields were also seen in previous examinations at the interim burnup of 2 at .%, but to a lesser extent. Examinations also showed W-UO_2 interaction characterized by an irregular W surface and an accumulation of metallic particles in the fuel. The metallic particles in the fuel are most likely W. No interaction was seen at the W-UO_2 interface in the examinations of the lower burnup samples. The W contained extensive porosity also not seen in the lower burnup samples. Examinations of the breach section of SU1-5 suggest a post-breach high temperature, consistent with xenon and krypton contamination of the helium and argon heat transfer medium in the emitter-to-collector gas gap. The breach may have initiated as a crack that was exaggerated by the over-temperature caused by the release of the fission gases.

Observations for specific fueled emitters are given below.

---

*Earlier PIE data are contained in Ref. 6-2.

TABLE 6-9

DESTRUCTIVE EXAMINATION MATRIX FOR THE UFAC-1B FUELED EMITTERS

EMITTER	SAMPLE	EXAMINATION
SU1-4	A	Longitudinal Metallography (LM)
	B	Retained Fission Gas (RFG)
	C	Transverse Metallography (TM)
	D	LM
SU1-5	A	LM
	B	TM
	C	Stored for future TM
SU1-8	A	RFG
	B	Burnup (BU)
	C	TM
	D	No examination chosen
SU1-9	A	RFG
	B	BU
	C	TM
	D	No examination chosen

Emitter SU1-4: The fuel structure shows the normal mature columnar grain structures expected for the high surface temperature UO_2. High magnification photographs of the UO_2-W interface show intimate contact and definite interaction, with transport of metallic W into the fuel. The W also showed significant porosity.

Three metallography samples were examined from emitter SU1-4. Sample A showed extensive interaction in the lower heat shield region and observable emitter deformation. The appearance of metallic reaction products suggest a once molten eutectic formation with the emitter, heat shield material, fuel, and fission products.

The interaction at the bottom end, in the area of the heat shield, was seen in the examinations at the interim burnup level (Ref. 6-2), but the interaction at 2 at .% was much less. The examinations of companion emitters at 2 at .% did not show any interaction of the UO_2 and W away from the heat shield and no porosity in the W.

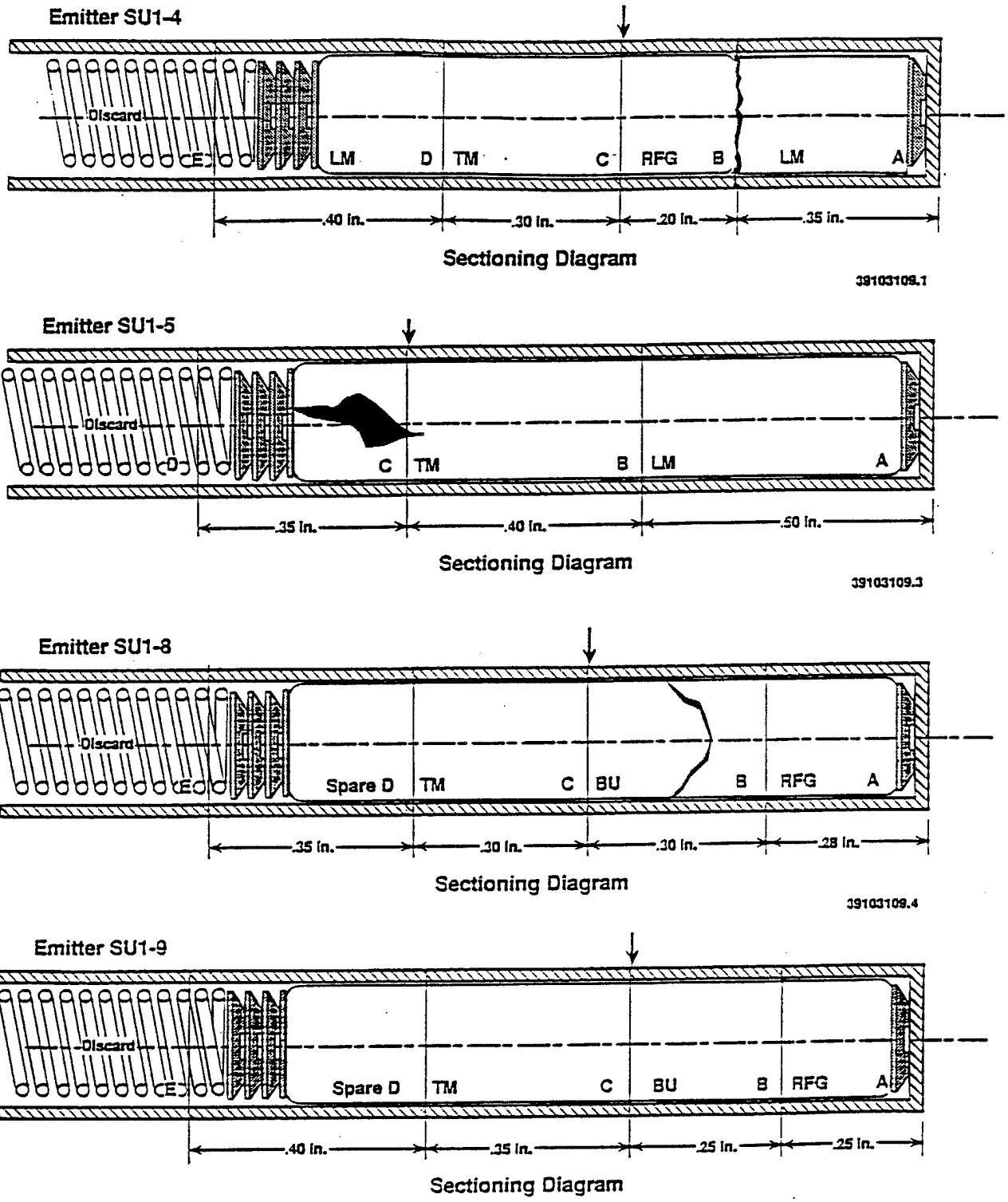

Figure 6-6. Sectioning Diagrams for UFAC-1B Fueled Emitters

The transverse sample removed at the center of the fuel column (Sample C) showed similar UO_2 and W interaction. Sample C had an incipient crack in the W emitter. The examination suggested the crack either occurred after irradiation or did not penetrate all the way through during irradiation since there were no changes in the fuel structures near the crack compared to the rest of the sample. The crack appeared to be decorated with porosity which may not be real, but the result of microcracking and sample fallout during preparation.

Sample D removed at the top of the fuel column also showed UO_2-W interaction similar to that seen at the bottom of the fuel column, but to a lesser extent. Fuel grain structures at the top of the fuel column were very similar to those seen at approximately half the burnup. The UO_2-W interaction at the top of the fuel column appeared to be very similar to that seen at the bottom of the emitter. The W interaction in the areas opposite the top heat shields and spring was less than in the area opposite the fuel. The W also shows little or no porosity in the area opposite the heat shields where the emitter temperatures decrease rapidly to approximately 1200 K.

Emitter SU1-5: Three metallography samples were removed from SU1-5 for examination and two were studied. The longitudinal surface of the Sample A was obtained by removing approximately 10% of the diameter of the sample to just expose the fuel. The longitudinal surface usually examined corresponds as closely as possible to the center of the sample, i.e., 50% of the diameter. The surface exposed provided a unique perspective looking directly down the temperature gradient on the UO_2 columnar grain structure in the outer region of the fuel. The W showed extensive porosity and interaction in the area of the lower heat shield, similar to that seen in SU1-4 Sample A. The characteristics and extent of the interaction was very similar to that seen in SU1-4. Fuel structures were regular with no unusual structure formation. The extent of UO_2-W interaction was also very similar to SU1-4.

Sample B showed the lower portion of the axial breach. The breach was very typical of an encapsulated pin breach where the capsule thermal bond was gas rather than liquid metal. The reduction in gap gas conductivity, due to the intrusion of the fission gases Xe and Kr into the He and Ar mixture, would increase the emitter surface temperature and compounded the breach. Therefore, the postirradiation character of the breach does not represent the initial appearance. The breach may have initially been a crack extending through the emitter resulting from UO_2-W interaction and a porosity accumulation in the W. The release of fission gases would have blanketed the area of the breach, raised the emitter surface temperature, and resulted in a breach which appeared characteristic of a gas pressure loaded failure.

The UO_2 in the open breach area contained several metallic inclusions which may be the result of the over-temperature and not UO_2-W interaction at normal operating temperatures. The W in the area of the breach showed a significant thinning and loss of material. This material loss may be the result of the over-temperature, or could be the result of some material loss during sample preparation.

The temperature increase across the fuel during operation was approximately 400 K. Since the fuel structures showed no evidence of fuel melting, fuel center temperatures were less than approximately 2700 K. Therefore, fuel surface temperatures could be as high as 2300 K in the area of the breach. This corresponds to an approximate 500 K over-temperature in the vicinity of the breach, a consequence of the intrusion of the Xe and Kr into the gas-gap. These over-temperatures are consistent with calculated decreases in gas conductivity with the inclusion of Xe and Kr into a He and Ar gas mixture.

The extent of UO_2-W interaction away from the breach location was minimal and appeared to be very similar to the interaction in SU1-4. This suggests the apparent over-temperature was localized.

Emitter SU1-8: One metallography sample was removed at the approximate center of the fuel column. Sample C showed a large well formed center void with columnar grains extending to near the UO_2-W interface, consistent with the previous samples examined. The UO_2 showed the large concentration of metallic inclusions seen in the previous samples. The interaction at the UO_2-W interface is similar to the previous samples examined. The emitter showed extensive porosity.

Emitter SU1-9: One metallography sample was removed at the approximate center of the fuel column. Sample C showed a large central void with fuel structures consistent with expected performance and the previous samples examined. The extent of UO_2-W interaction was also very similar to the other samples examined at this burnup.

Electron Microprobe Examination: Shielded electron microprobe examinations of the SU1-4 sample A were made in 3 general areas as shown on Fig. 6-7: the intersection of the W emitter and lower W/Re heat shield (locations 1 and 3), the area below the W/Re heat shield showing the presence of a once molten reactor product (location 2), and the W emitter-UO_2 interface (locations 4 and 5).

The major constituent, other than W and Re, at the intersection of the heat shield with the emitter was U. The U appeared in the reactor product zone at the interface. There was no migration of Re out of the W/Re heat shield. Fission products were not found in the area in significant concentrations.

The metallic reaction product in the area between the bottom of the emitter and the heat shield was primarily W. A narrow band of U was found next to the W emitter reacted inner surface. Again Re was only found in the heat shield and no other fission product metals were detected.

At the W emitter-UO_2 fuel interface, the fuel and emitter are in firm contact

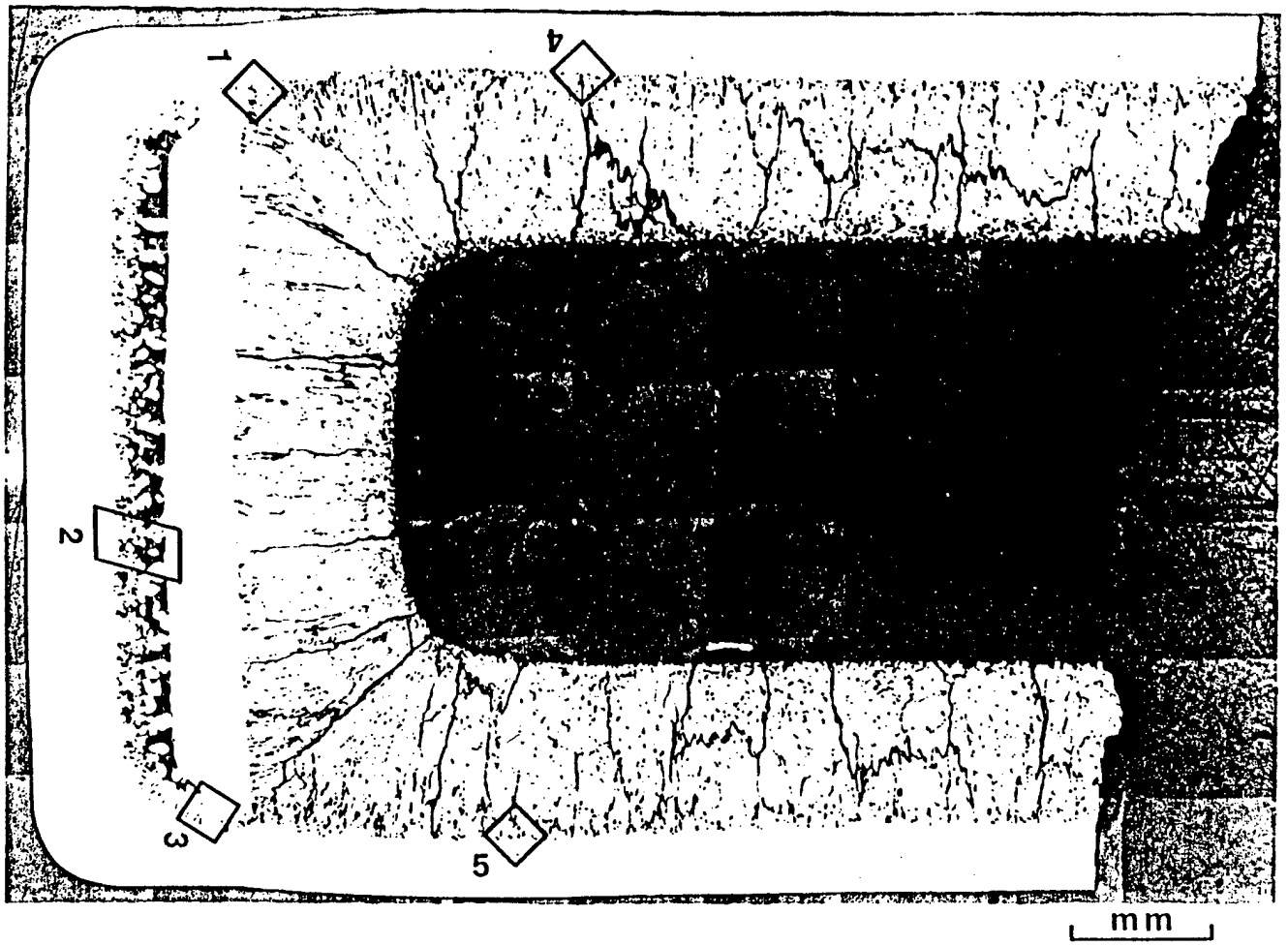

Figure 6-7. UFAC-1 Examinations. Areas on sample SU1-4A examined with the shielded electron microprobe.

interface. There were however, metallic particles in the fuel. These particles were predominately W with a few percent Mo most likely fission product Mo.

Apparent second phase inclusions in the emitter were examined and found to contain only W. The microprobe was set to detect elements with an atomic number 14, i.e., silicon or higher. Osmium was found in low concentrations in the W/Re heat shield.

Conclusions: One emitter, SU1-4, breached during irradiation and limited examinations of the breach section suggest a local over-temperature in the vicinity of the breach.

All four emitters were fractured in the region of the W-Ta transition at the top of the emitter. Examinations of the fractures showed them to be very similar to the fractures that occurred in the emitters examined at about 2 a/o burnup. The high fluence W was very brittle at ambient temperatures and fractured in the fuel column during routine handling during the examination.

Metallography samples removed at the bottom of the fuel column showed extensive interaction of the W emitter with the W-Re heat shield and the UO_2 fuel. This interaction, which may have contributed to the breach, was also seen during the interim examinations, but to a lesser extent. Postirradiation structures suggest that a low melting temperature eutectic was formed. A microprobe examination indicated uranium to be present at the intersection of the W/Re heat shield and the emitter. W was found between the bottom of the heat shield and the bottom of the emitter.

The W and Mo observed dispersed in the fuel probably resulted from the fabrication process. Milling materials contain W and Mo and it would not be surprising to have 50 to 100 ppm W or Mo introduced into the UO_2.

Examinations, with the exception of the breach, did not show any evidence that the fueled emitter lifetimes were exceeded by irradiation to goal burnups of 4 at .%. Postirradiation fuel structures were consistent with expected operating temperatures. The problem of interaction in the area of the W and the W-Re heat shields has been eliminated by the replacement of W-Re with W as heat shield material for future designs.

6.4.2 UFAC-2 Status

UFAC-2 contains 2 real time fueled emitters from Batch 1 and 4 from Batch 2. UFAC-1C completed irradiation at the end of Run 158 and as of April 1 are awaiting interim examination and reconstitution into UFAC-2D. Interim examinations include disassembly and removal of the capsules, visual examinations, dimensional measurements, capsule weights, and neutron radiography. Irradiation will resume in mid-May with Run 160. The fluence and burnup accumulated to date are shown in Table 6-4.

6.4.3 UFAC-3

UFAC-3 contains 2 accelerated emitters from Batch 2, SU3-16 and SU3-18. These fueled emitters reached a burnup of 2.8 a/o and 3.5 a/o, respectively, and were removed for final PIE after Run 158.

Examinations at ANL-W will include visual examinations, dimensional measurements, neutron radiography, and detailed axial gamma scans of the fueled emitters. They will then be sent to WHC for destructive PIE.

References

6-1 Paxton, D. M. and L. A. Lawrence, "Irradiation and Examination of the UFAC-1B Fueled Emitters", WHC-SP-0698, September 1991.

6-2 Makenas, B. J., et al., "Interim Examinations of UFAC-1 and UFAC-2 Fueled Emitters", WHC-SP-0519, April 1990.

7. CESIUM RESERVOIR AND INTERCONNECTIVE TFE COMPONENTS

7.1 OBJECTIVE

The overall objective of the cesium reservoir and interconnective TFE components task is to develop and validate the performance of cesium reservoirs and interconnective TFE components, such as intercell insulation, fission product vents and fission product traps. In particular, the objectives are:

1. Design integral cesium reservoirs and interconnective TFE components.

2. Develop required fabrication processes for integral cesium reservoirs and interconnective TFE components and document the process specifications.

3. Fabricate integral cesium reservoirs and interconnective TFE components for in-reactor and ex-reactor tests.

4. Verify the performance characteristics and lifetimes associated with integral cesium reservoirs and interconnective TFE components by means of in-reactor and ex-reactor testing.

5. Develop an analytical model of the performance and lifetime of the Cs reservoir and interconnective TFE components.

7.2 TASK DESCRIPTION

The integral cesium reservoir and interconnective TFE tasks consists of five subtasks:

1. Cesium reservoir and interconnective TFE components design. Design integral cesium reservoir test specimens consistent with the TFE design

requirements. Design test specimens of intercell insulation and interconnective TFE components such as TFE end restraint and fission product traps, ports and tubes consistent with TFE design requirements.

2. Fabrication development. Determine integral cesium reservoir materials with the capability for storing cesium either as intercalation compounds or as sorption reservoirs. Develop systems for containing the integral reservoir material in a TFE environment. Select insulator materials such as Al_2O_3, Y_2O_3 and YAG and develop processes for fabricating TFE end restraints and intercell insulation components. Develop materials for use as fission product traps and develop components for fission product vent and port tubes.

3. Ex-reactor testing. Perform ex-reactor tests to determine the cesium pressure of integral reservoir materials as a function of cesium loading and temperature. Examine the ability of intercell insulation coatings to reduce parasitic discharges. Determine the mechanical stability of TFE end restraints.

4. In-reactor testing. Determine the effect of fast neutron fluence on the stability of the pressure versus temperature characteristics of integral cesium reservoirs at a fixed cesium loading. Also examine the mechanical stability of prototypical TFE end restraints and intercell insulation coatings. Determine fission product release characteristics from the fuel and evaluate the effectiveness of the fission product control components and assemblies.

7.3 PROGRESS DURING PRESENT REPORTING PERIOD

In the present reporting period the cesium reservoir model has been reexamined in light of the UFAC-3 PIE results reported in the last semiannual (Ref. 7-1). In those measurements, there is little change in the Cs pressure reservoir temperature isostere of Cs intercalated POCO graphite resulting from exposure to a fluence of $3x10_{22}$ n/cm^2. The neutron radiographs taken after the irradiation show both graphite samples to be fragmented. X-rays taken after intercalation, but prior to final encapsulation at the reactor site (and, therefore, prior to irradiation), show the graphite discs to be intact, though there is a volumetric swelling of about 46% for sample 960D and about 72% for sample 929D due to the cesiation. There is no direct evidence that the fracture of these two POCO graphite samples occurred as a result of neutron irradiation. During the preparation and characterization of samples for the subsequent UCA-3 series of tests, the friability of cesiated graphite was inadvertently demonstrated. The UCA-3 specimens were observed to be fragmented in the preirradiation x-rays and the cause was traced to a documented jarring accident in the electron beam welder when the final pinchoff was bead-welded. From that experience, it is inferred that the mechanical condition of the present samples is due to a similar impact that occurred, but was not documented, during handling at the reactor site. There is, at present, no reason to suggest that the fracture is more likely to have occurred before, rather than after the in-core irradiation.

In contrast to the results with POCO, the vapor pressure of Cs over HOPG is much lower after irradiation to a fluence of $0.9x10^{22}$ n/cm^2. The pre- and postirradiation isosteres are nearly parallel, indicating that the dominant effect of the neutron fluence is characterized by a change in the entropy term of the equilibium reaction. It is also important to note that a temperature error alone would not cause the observed difference. The extreme distortion of the HOPG sample seen in the neutron radiograph has been discussed previously as an effect of the pleated-layer model of Cs-graphite intercalation compounds. In that model, the cesium exists in

domains, or islands inthe galleries between graphite layer planes. The boundaries of these islands act as nucleation sites for knock-on atoms, thereby promoting the formation of new graphite planes. The environment of the Cs islands will thus be altered, since the new graphite planes will have holes at each island. As the damage progresses, ie., as the number of new planes increases, a cylindrical void volume may tend to be formed at each island. The diameter of the volume will be less than that of the original island due to the attendant a-axis shrinkage. Some redistribution of Cs between the newly formed planes can be expected, but it is probably not enhanced by the neutron irradiation, due to the much less efficient transfer of momentum in cesium as compared to carbon. The final configuration of the Cs-graphite compound may be envisaged as a structure that contains cylindrical 'caverns' of various axial heights; the 'tallest' being remnants of the original 'islands'. The outer edge of the specimen can be expected to have a more normal intercalation structure, since it is in equilibrium with cesium vapor throughout the irradiation.

Considerable distortion of the tantalum end caps is observed in the neutron radiograph of the HOPG sample, indicating that the HOPG graphite was under pressure during the latter part of the irradiation. The magnitude of this pressure can be estimated from the dimensional changes of the end caps. Such an estimate yields a force on the graphite of less than about 230 psi (16 bar). The application of a pressure in the kilobar range (in the c-axis direction) has been shown to increase the staging of intercalated graphite. It is not likely that this effect played a role in the present results.

A rationalization of the disparate results of the present POCO and HOPG Cs pressure tests may involve the influence of the edge planes of the two samples. For the HOPG sample, the edge plane area is equal to the area of the edge of the disc, about .45 cm^2. POCO graphite may be viewed phenomenologically as arrays of aligned HOPG crystallites contained in an isotropic distribution of small grains. In this view, the edge plane density is related to the grain diameter. For grain diameters

ranging from 1 to 10 M in the a-axis direction, the exposed edge plane area is a factor of 10^{3-4} larger in the POCO specimen, or about 450 to 4500 cm^2. The amount of Cs contained in the edge region may be estimated in the following way: if this region is characterized by a thickness equal to a typical island diameter of 300 A, then a little less than 0.01 moles and between 10 and 100 moles of cesium is contained in the edge plane region of the HOPG and POCO samples, respectively. The test fixture in which the pressure vs temperature isosteres were measured has a volume of about 300 cm^3. From the gas law, 3 mole of cesium is required to establish a pressure of 1 torr. Thus, in the case of the POCO sample, the measured isostere is characteristic of this edge region, whereas for the HOPG sample, this region is completely depopulated and the isostere is representative of the interior of the sample.

In the UCA-2 test (Ref. 7-2), for the single POCO sample studied, the postirradiation isostere intersected the isostere obtained upon initial laboratory characterization at a temperature of about 1060 K. At higher temperatures, the postirradiation isostere was characterized by higher pressures: at 1150 K, the PIE pressure was 5 torr, whereas it had been between 2 and 3 torr after initial loading. Furthermore, this POCO specimen was intact after irradiation; it had undergone a 14% volume reduction, bringing the final volume back to the preintercalation volume. These volume changes in POCO were correlated with the corresponding changes in HOPG by assuming that the crystallites had a large aspect ratio (a-axis diameter to c-axis height) (Ref. 7-3). The condition of this earlier POCO sample suggests that it was not subjected to the same inadvertent acceleration as were the samples in the present tests.

The three different results discussed above can be included within the framework of the same qualitative model if it is presumed that the fracture of the present POCO samples occurred prior to irradiation. Then, both the HOPG and POCO samples of the present work are characterized by a quasi-normal edge region enclosing an interior region comprised of cesium 'caverns' of various sizes,

interspersed by a few cesium islands. The HOPG isostere samples this inner region, whereas the POCO isosteres sample the edge region. In the UCA-2 test, the edge regions of the individual crystallites were exposed to a different physical environment during irradiation. The mechanical restraints imposed by the presence of the adjacent crystallites could have resulted in the formation of a different structure and, therefore, a different thermodynamic behavior, as was observed. On the other hand, if the present POCO samples been fractured after irradiation, it would be difficult to explain why their isosteres differed from that of the UCA-2 sample.

In the next reporting period these qualitative ideas will be incorporated into the Cs reservoir model, pending modification by subsequent PIE data.

References

7-1 TFE Verification Program Semiannual Report for the Period Ending September 30, 1991, GA-A20804, December 1991.

7-2 TFE Verification Program Semiannual Report for the Period Ending April 30, 1989, GA-A19666, September 1989.

7-3 TFE Verification Program Semiannual Report for the Period Ending March 31, 1991, GA-A20493, April 1991.

8. THERMIONIC FUEL ELEMENT

8.1 OBJECTIVE

The overall goal of the thermionic fuel element task is to demonstrate that TFEs prototypic of a 2 MW(e) thermionic space nuclear power system of seven year life can be fabricated from well modeled components, and that their performance is as predicted when operated in a prototypic thermionic reactor environment. Derivative goals include:

1) Produce a TFE engineering design and specification.
2) Develop required TFE assembly processes, process specifications, and demonstrate manufacturing capability.
3) Fabricate TFEs and test them to demonstrate the processes and the integrated performance of the components.
4) Develop and verify a TFE model that can predict TFE performance and lifetime.

Components with demonstrated performance and which are projected to meet lifetime requirements will be used in these TFEs. The performance of one prototypic TFE will be demonstrated in EBR II. Thermionic fuel elements leading up to the prototype will undergo irradiation in the General Atomics Mark F TRIGA reactor.

8.2 TASK DESCRIPTION

8.2.1 Testing Logic

All converters tested in the TFEs will be of the baseline configuration. The balance of the test article will be as close to the baseline TFE design in geometry and performance as practicable. Test and design requirements are compared in Table 8-1.

The separate in-reactor tests and the distinctions between them are outlined in Table 8-2. Note that tests 3H2 thru 3H4, which were originally proposed, have been deleted.

TABLE 8-1

COMPARISON OF TFE TEST REQUIREMENTS WITH SYSTEM BASELINE DESIGN REQUIREMENTS

	TFE Test Requirements (BOL)	Baseline Design Requirements (BOL)
Converter power density average (W/cm^2)	3.4	3.4
Current density average (A/cm^2)	7	7
Emitter temperature average (K)	1800	1800
Collector temperature average (K)	1070	1070
Sheath-collector voltage maximum (V)	7.5	7.5
Converter configuration	Baseline	Baseline
TFE materials	Baseline or variants for performance structural improvements	Section 2
Fuel enrichment (% U-235)	Variable enrichment	93: variable fuel volume fraction
Fast fluence: nominal (E>0.1 Mev)	Real time	$2.7x10^{22}$/ 7 years
Fuel burnup: nominal (a/o)	4.1	4.1
Cesium reservoir type	Variable with test	Integral graphite
TFE environment/heat sink	Helium/test reactor coolant	Liquid metal (Li)
Reflector above/below within TFE	No	Yes
Reactor vessel penetration integral with TFE	No	Yes

The logic behind this test series is a step-by-step development of the fabrication processes, culminating in the fast reactor prototype. The first step is the development of the processes for a single cell, and the integration of the single cell into a TFE sheath tube with appropriate end fittings. These end fittings involve the cesium

TABLE 8-2

TFE IN-REACTOR TEST SUMMARY MATRIX

TFE ID	Fuel/Emitter Collector	Cs Reservoir	Purpose	Reactor
1H1	UO_2/W/Nb	Pool	Verification of reference cell design performance and fabrication processes. Sheath integration.	TRIGA
1H2	UO_2/W/Nb	Graphite	Verification of integral cesium reservoir design, performance.	TRIGA
1H3	UO_2/W/Nb	Pool	Study effect of fission products mixing with cesium.	TRIGA
3H1	UO_2/W/Nb	Graphite	Intercell process development. Fission product control.	TRIGA
3H5	UO_2/W/Nb	Graphite	Backup to 3H1. Introduction of prototypic components outside cell.	TRIGA
6H1	UO_2/W/Nb	Graphite	Verification of long-TFE fabricability.	TRIGA
6H2	UO_2/W/Nb	Integral Graphite	Backup to 6H1. Introduction of prototypic components.	TRIGA
6H3	UO_2/W/Nb	Integral Graphite	Verification of TFE performance in fast reactor environment.	TBD

reservoir, fission gas venting and the conduction of electrical current produced. This single-cell TFE is designated "1H", where the H refers to the latest generation of thermionic cell in a megawatt class TFE, and the "1" refers to the number of cells in the TFE.

The second step is the development of the intercell region of the TFE. The test vehicle will be the 3H-series TFE which will contain three of the H-series cells welded end-to-end in an electrical series circuit. The center cell in the series is isolated from TFE end-fittings and is thereby typical of cells within the interior of a thermionic reactor. The testing of the three cell TFE also allows the study of fission gas venting in a representative multicell environment at a minimum expense.

As the last step in the testing before the fast reactor prototype test, 6H-series TFEs will be built to demonstrate the fabricability of a long TFE where axial alignment is critical. Testing of these TFEs will provide additional demonstration of fission product venting and the capability to maintain unobstructed fission gas passages.

Success in the process development will be evidenced by the observed in-reactor performance and stability.

The following materials and/or components are used in all TFEs:

- o Insulator crystal state: polycrystalline
- o Emitter body material: W from WF_6
- o Emitter surface material: W from WCl_6
- o Emitter stem material: W from WF_6
  - Length: .43 in.
  - Thickness: .020 in.
- o Collector material: Nb
- o Emitter transition material: tantalum.

Other TFE features that vary are shown on Table 8-3.

8.2.2 TFE Design

The TFE design has been described in previous semiannual reports (Ref. 8-1). The H-series thermionic converter design is as illustrated in Fig. 8-1, and the representative TFEs for TRIGA test are pictured in Fig. 8-2.

8.2.3 TRIGA Facility

The Mark F TRIGA reactor at General Atomics will be used for most TFE testing. TRIGA is a water-moderated pool-type reserach reactor. The Mark F includes a neutron radiography facility located within the reactor pool for periodic nondestructive diagnostic examinations of the TFE internals. A hot cell at the site provides capability for postirradiation examination.

TABLE 8-3

TFE TEST MATRIX

	1H1	1H2	1H3	3H1	3H5	6H1	6H2	6H3
Emitter cap material	Ta	Ta	Ta	Nb				
Flight fuel holddown	No, use spring						Yes	
Volatile fission product trap								
Location	Vac		Cell					
Material	-		Al_2O_3					
Optimized design	-		No				Yes	
Trilayer								
Insulator	Y_2O_3	Al_2O_3						
Square or shaped ends	Square						Shaped	
Ceramic-to-metal seal								
Insulator	Al_2O_3							
Configuration	Litton						Trilayer	
Emitter alignment								
W/Re spring	Belleville			Cylindrical Spring				
Insulator	Solid Al_2O_3			Planar Al_2O_3 Trilayer				
Configuration	2 piece			Trilayer in Cap				
Cesium reservoir material	Liquid	POCO	Liquid	POCO				
Fuel pedestal, material design	W/Re				W			
Top of converter string								
Bus bar material	Nb				Nb/Mo			
Lead trilayer insulator	Al_2O_3							
Stem seal insulator	Al_2O_3							
Stem seal configuration	Litton						Proto	
Fission product port tube	Proto							
Vessel head penetration	Not applicable						Proto	
Dummy reflector block	Not applicable							
Bottom of converter string								
Dummy cell	Yes		No		Yes	No		
Dummy reflector block (and positioner)	Not applicable							
TFE alignment pin	Not applicable							

The TRIGA typically operates at about 1.4 MW(t). At this power level, the fast fluence is about 1×10^{21} nvt (E>.1 Mev) per year.

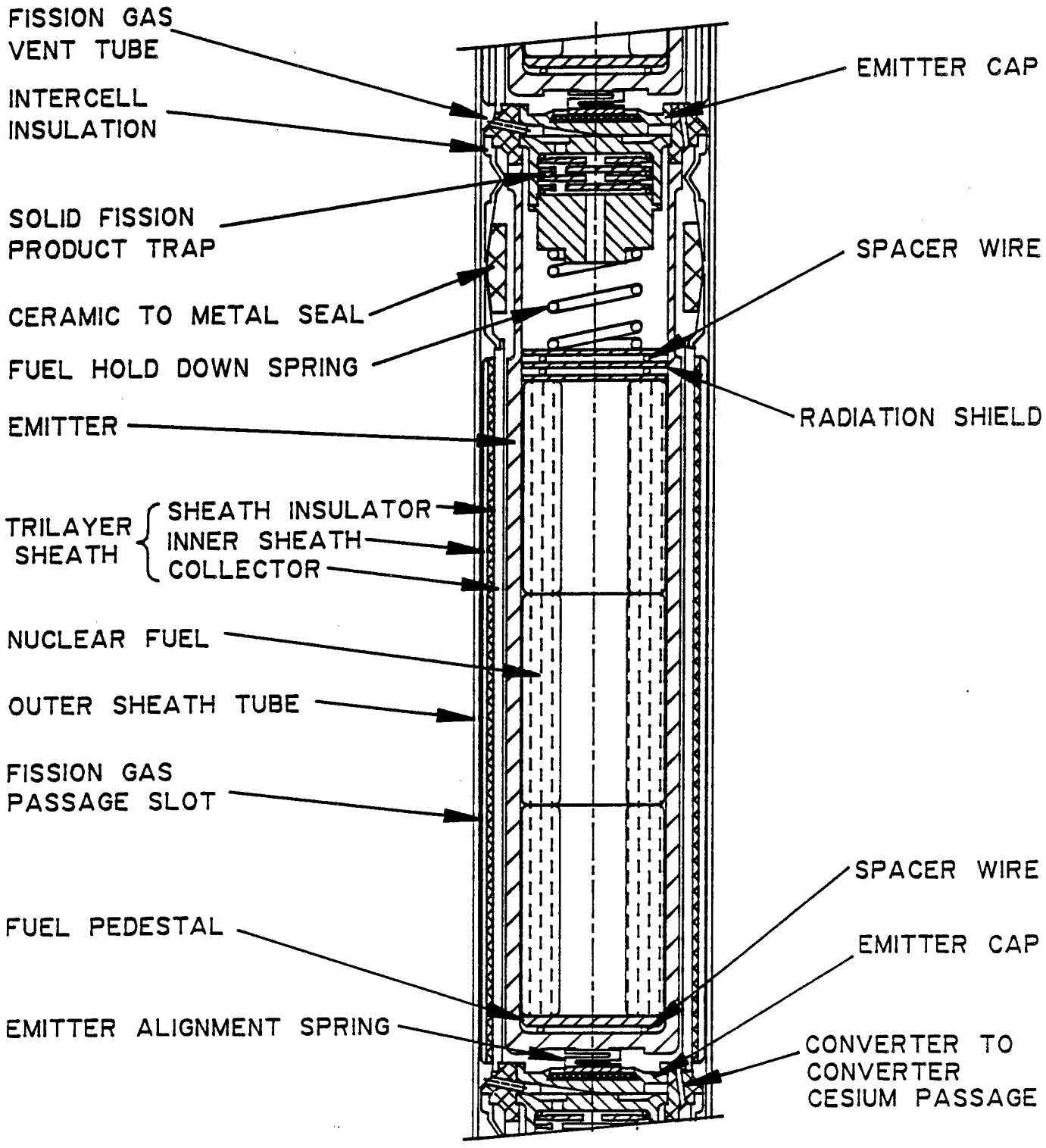

Figure 8-1. H-series thermionic converter (typical of 3H1)

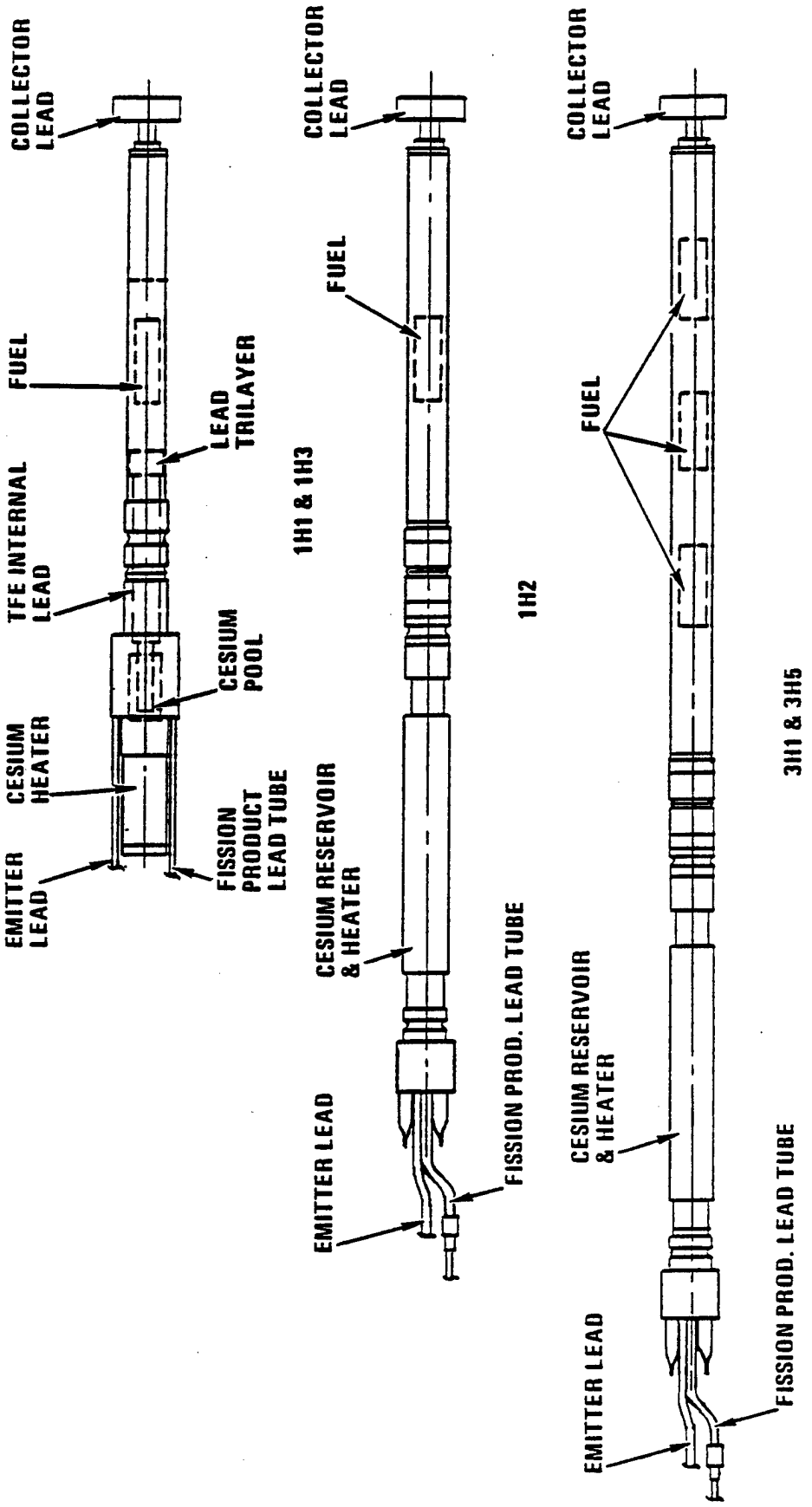

Figure 8-2. TFEs for TRIGA test

8.3 TFE TESTING

8.3.1 TFE Operations

The status of TFE irradiations in TRIGA as of April 1, 1992 is shown below:

	1H1	1H2	1H3	3H1
Test hours	17,200	14,000	19,500	7,000
Output voltage, volts	-	-	.37	1.43
Output current, amps	-	-	.04	64

TFE-1H1 was removed from the core in December, 1990 and is undergoing PIE.

8.3.2 TFE-1H1

Background: The operating history of TFE-1H1 was reviewed in Ref. 8-2 and earlier semiannual reports. Briefly, a loss of electron cooling incident during startup led to an over-voltage across the cell and a 600 watt arc sustained for at least 20 sec. The resulting temperature excursion when combined with the arc led to a reduced but steady output, characteristic of a low resistance, parallel electrical path within the cell.

An electrical schematic of 1H1 is shown on Fig. 8-3. It is postulated that the low resistance path within the TFE could be due to damage of the stem ceramic-to-metal seal, the emitter lead trilayer sheath insulator or the converter ceramic-to-metal seal.

Postirradiation Examinations: TFE-1H1 was removed to the hot cell in November, 1991 and is currently undergoing PIE. Preliminary resistance measurements have not indicated any damaged insulators. However, the following additional checks are underway:

1) Inspection of the centering insulator at the bottom of the collector.
2) Search of the environs for a conductive path.

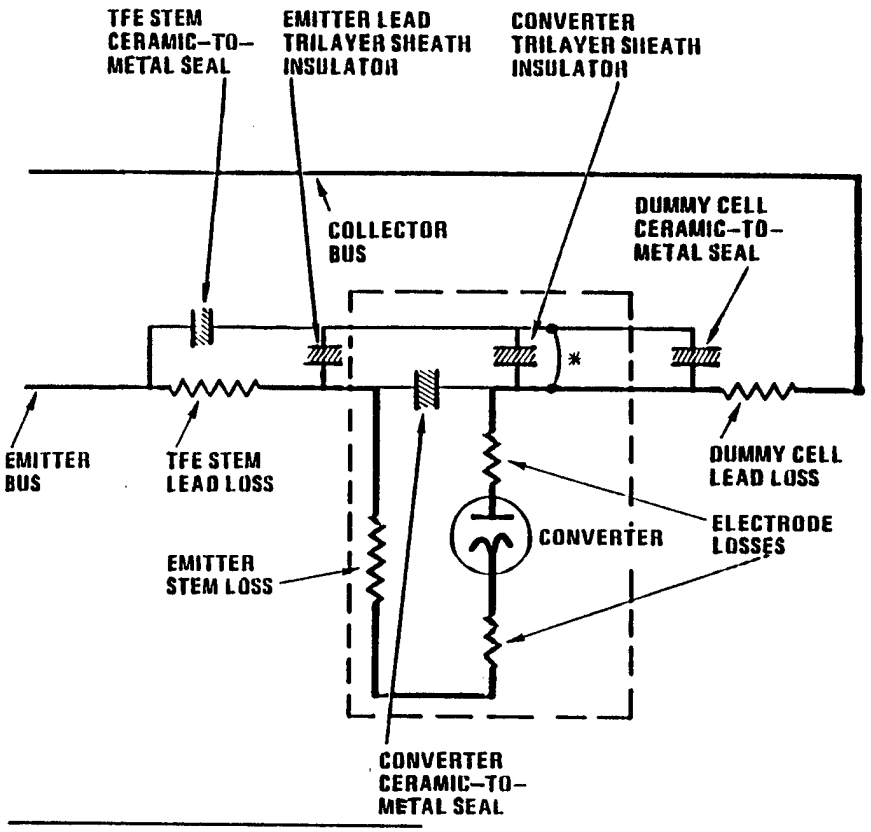

* Shorted during fabrication

Figure 8-3 - 1H1 Electrical Schematic

When these are completed, the test specimen will be shipped to WHC for further PIE. Discussions with DOE-SAN indicate an environmental assessment may be required for the shipment from GA and WHC. Existing NEPA documentation at WHC covers the receipt and handling of the shipments. GA is responsible for obtaining the necessary approval, scheduling the appropriate cask and truck, and shipping the test article to WHC. WHC is responsible for obtaining approval to receive the shipment, cask unloading and terminal examination of the emitter and collector.

Options for examining the emitter and collector surfaces for contaminates such as uranium are being evaluated at WHC. LANL has the capability to do auger microprobe examinations and secondary ion mass spectrometry on the collector surface if the sample radiation levels are no more than 1R at contact. Measurements of the radiation levels of the UCA-1 sheath insulator samples suggest that reducing

the size of the sample to approximately 0.5 inch by 0.5 inch will reduce the radiation to an acceptable level. Other techniques such as an acid etch of the emitter surfaces with subsequent analysis of the acid bath for uranium are being evaluated for the emitter.

8.3.3 TFE-1H2

Background: As outlined in Ref. 8-1, the loss of a cesium reservoir heater in June, 1991, caused an over-voltage in the TFE and the apparent short of the emitter lead sheath insulator. The test history for the previous 9000 hours had been very stable.

The June, 1991 incident developed as follows:

1) The auxiliary cesium reservoir heater failed causing a drop of in the reservoir temperature.

2) This caused a drop in the cesium pressure decreasing the cesium coverage of the emitter. As a result, the emitter was unable to supply the current demanded by the power supply.

3) In response to the power supply, a potential gradient developed at the emitter forcing cesium ions onto the surface.

4) The resulting ion bombardment caused the temperature of the emitter to increase, driving off still more cesium, and a thermal excursion resulted.

5) A scram did not occur since it had been bypassed for diagnostic reasons.

The duration of the excursions was less than 4 minutes. Conditions recorded by the data acquisition system were as follows:

	Normal	During Excursion
Collector temperature	800°C	1000
Top of Cs reservoir	640°C	610
Diode voltage	0.2v	-12.7 volts
TFE current	120 amps	90

The actual extreme values for these parameters could have been more severe since the recording rate of the data acquisition system was not fast.

Status of 1H2: TFE-1H2 remains in the reactor. Efforts have been made to clear the short by burning it out with power supply current, the actual process being based on the circuit analysis. Those efforts were not successful.

Other means for clearing the short are being studied, namely:

- o A high short-duration voltage pulse.
- o High external current.

If the short cannot be cleared, 1H2 will be removed from the core.

8.3.4 TFE-1H3

Background: As shown in Table 8-2 the unique feature of 1H3 is that the fission gas space above the UO_2 in the emitter can communicate with the cesium filled interelectrode gap. The purpose of the test is to measure the degradation in thermionic performance as fission gases enter the interelectrode gap. A schematic picture of the 1H3 cell is shown on Fig. 8-4.

Small changes in performance were observed during the first 12,400 hours of operation. Then, performance began to degrade.

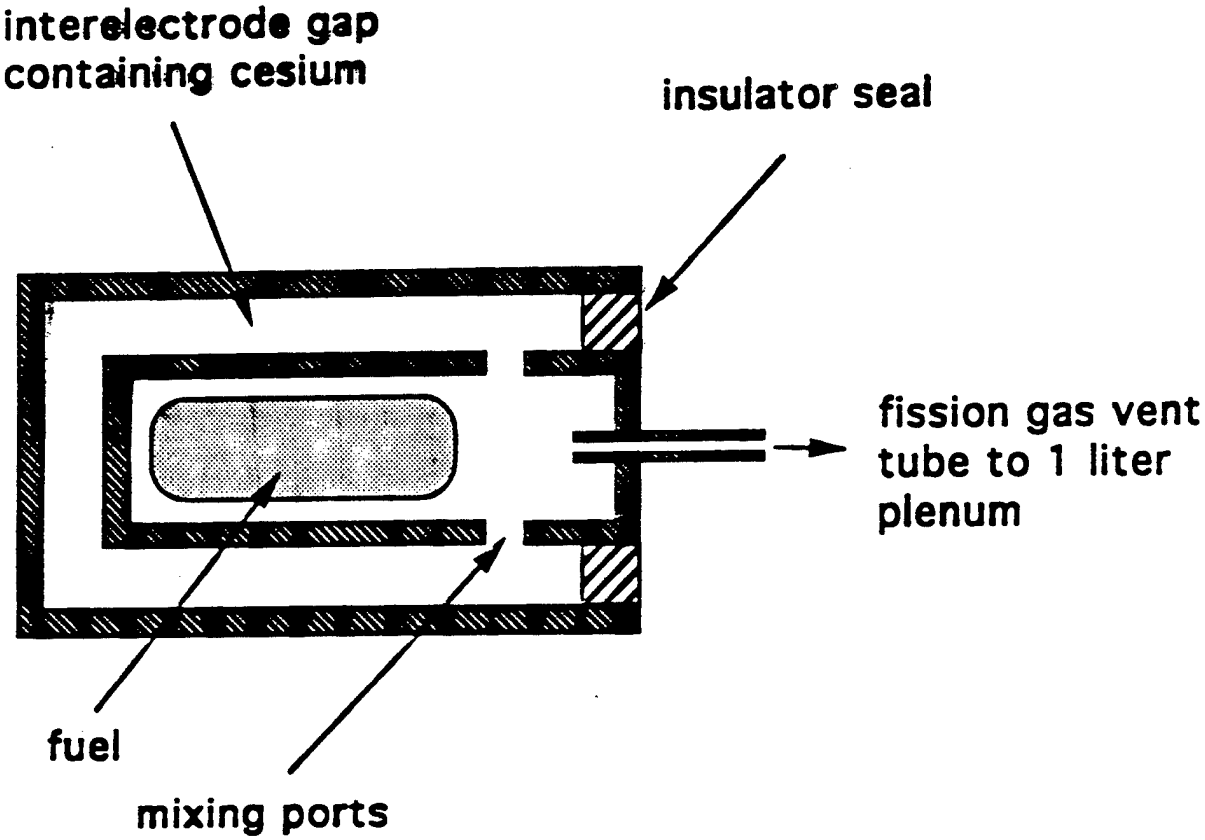

Figure 8-4 - Schematic Diagram of TFE-1H3 Schematic

An analysis of this degradation was presented in Ref. 8-1, from which it was concluded that a high fission gas pressure probably existed in the interelectrode gap. Possible effects of high gas pressure include:

1) Enhanced emitter cooling:
   - Reduce emitter temperature about 100°K
   - Reduce output voltage about .2 eV.
2) Plasma scattering:
   - Reduce output voltage about .2 eV.

The presence of high gas pressure (several hundred torr) in the interelectrode gap is indicated by the slow thermionic response to a change in cesium pressure in the reservoir.

It has been postulated that the fission gas vent tube to the one liter plenum is plugged. In order to prevent the Cs in TFE-1H3 from escaping into the fission gas plenum, this fission gas vent tube was fabricated with a smaller than normal ID of 0.002". In conventional TFE's, where the Cs vapor does not communicate with the fission gas plenum, the ID of this fission gas tube is larger, and hence is less prone to plugging. Such a plug could cause the pressure buildup indicated by the analyses reported in Ref. 8-1 and summarized above.

However, the above pressure related effects do not appear to be able to drive TFE performance out of the power quadrant. Something like an increase in collector work function of .5 to .6 eV would be necessary to explain the observed result. Such an increase could result from collector contamination by, for example, uranium or fission product plateout.

Status of 1H3: TFE-1H3 remains in the reactor. Steps are being taken to clear the apparent blockage in the vent tube. If that is unsuccessful 1H3 will be removed from the core.

8.3.5 TFE-3H1

3H1 is operating stably, as shown in Section 8.3.1.

In November, 1991 a drop in 3H1 performance was observed. As described below, this was due to a combination of a high collector temperature and a low cesium pressure.

The sensitivity of TFE output to collector temperature is shown in Table 8-4: the voltage decreases about 0.5 eV if the collector temperature increases about 100 K. This sensitivity of TFE output to collector temperature appears excessive, however, so an analysis of the behavior of the cesium reservoir was made. It was found that the Cs pressure associated with the 3H1 graphite reservoir thermocouple,

TABLE 8-4

3H1 PERFORMANCE VS COLLECTOR TEMPERATURE

DATE	IRRADIATION TIME	OUTPUT		COLLECTOR TEMPERATURE (K)			
	(HOURS)	(A)	(v)	TOP	MID	BOT	AVE
10-16-91	3754	63.9	1.44	981	977	1071	1010
10-28-91	3982	61.6	.89	1077	1064	1162	1101
1-27-92	5691	63.6	1.40	931	949	1040	973
2-12-92	6026	70.4	1.41	988	1019	1037	1015

using the original out-of-core calibration obtained when the reservoir was loaded, was not consistent with the Cs pressure deduced from in-core I-V data. Pertinent data are shown on Table 8-5.

TABLE 8-5

3H1 Cs PRESSURE/TEMPERATURE RELATIONSHIP VS OUT-OF-CORE (EXPECTED) DATA

3H1 GRAPHITE RESERVOIR TEMPERATURE (°C)	Cs PRESSURE DEDUCED FROM OUT-OF-CORE P/T DATA (torr)	CESIUM PRESSURE DEDUCED FROM IN-CORE I-V DATA (torr)
712	3.7	0.9
721	4.5	1.0
731	5.6	1.3
741	7.1	2.4
751	-	2.8
761	-	3.4

For the indicated reservoir temperature, the pressure deduced from out-of-core P/T (graphite loading) data is shown in the middle column of Table 8-5. However, a comparison of 3H1 I-V curves with I-V data from out-of-core converters leads to cesium pressure estimates which are 3 to 5 torr less, as shown in the last column of Table 8-5. Due to the known temperature gradients which exist in the region of the reservoir, the Cs pressure calibration derived from the I-V sweeps is more reliable. Figure 8-5, which shows how the cesium reservoir is thermally balanced between the emitter and the heater block, demonstrates the origin of the temperature gradient. The low Cs pressure in 3H1 results from the fact that the graphite was loaded on a steep portion of the isostere; only a small loss of Cs, due to surface adsorption on the converter components, is required to cause a significant reduction of pressure as shown in Fig. 8-6.

As shown in Fig. 8-7, converter performance is much more sensitive to collector temperature at low cesium pressure than at high pressure. For 3 cells, the TFE voltage for a 100 K change in collector temperature (e.g., from 1000 to 1100 K) is about 0.45 volts for a 1.4 torr Cs pressure but only about .15 volts for a 4 torr Cs pressure. This is the cause of the reduced performance on 10-28-91 shown in Table 8-4.

Bottom Collector Temperature: As shown in Table 8-4, the bottom collector tends to run hotter than the upper two collectors. The reason is that insulating high density alumina tubes that protect thermocouples in the regions above the lower collector, and contribute to collector cooling, were not required at the lower collector because the thermocouples terminate at the upper collectors. This design feature can be corrected for 3H5. Without the radial thermal path provided by the alumina tubing, the bottom collector must operate at a higher temperature to reject its heat through gas gaps and into the TRIGA and water.

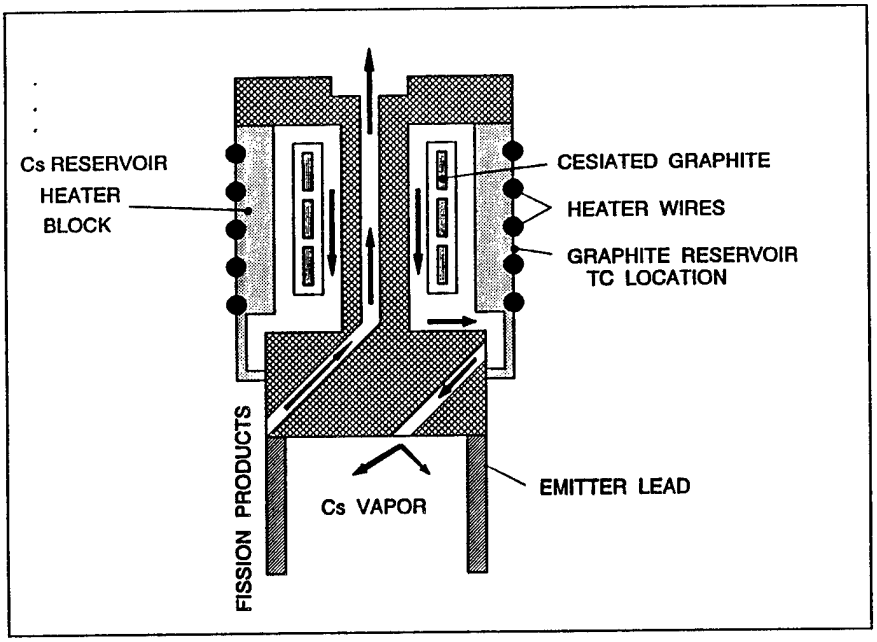

Figure 8-5 - Graphite Cs reservoir is thermally coupled to heater block - and also to emitter lead

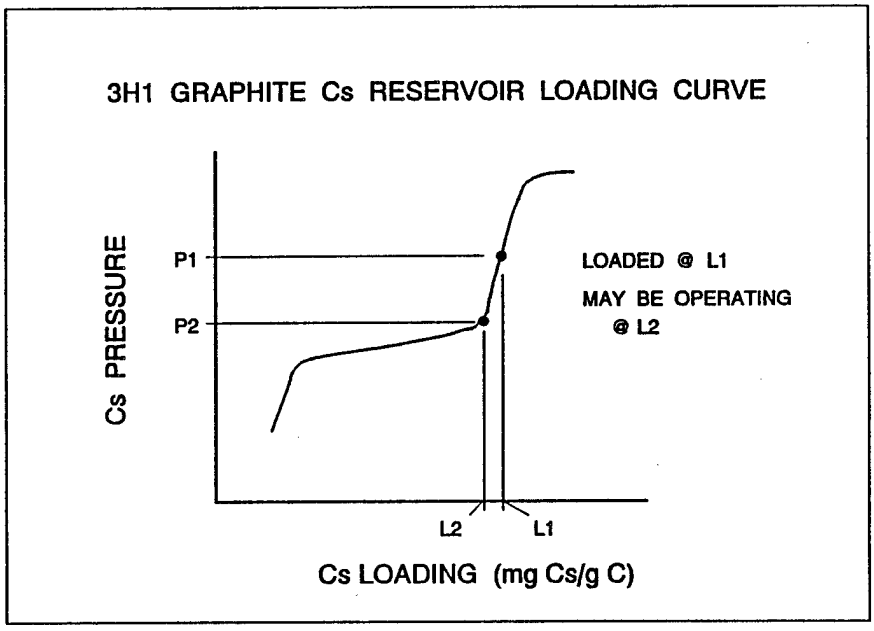

Figure 8-6 - Some Cs consumption could cause change in Cs pressure

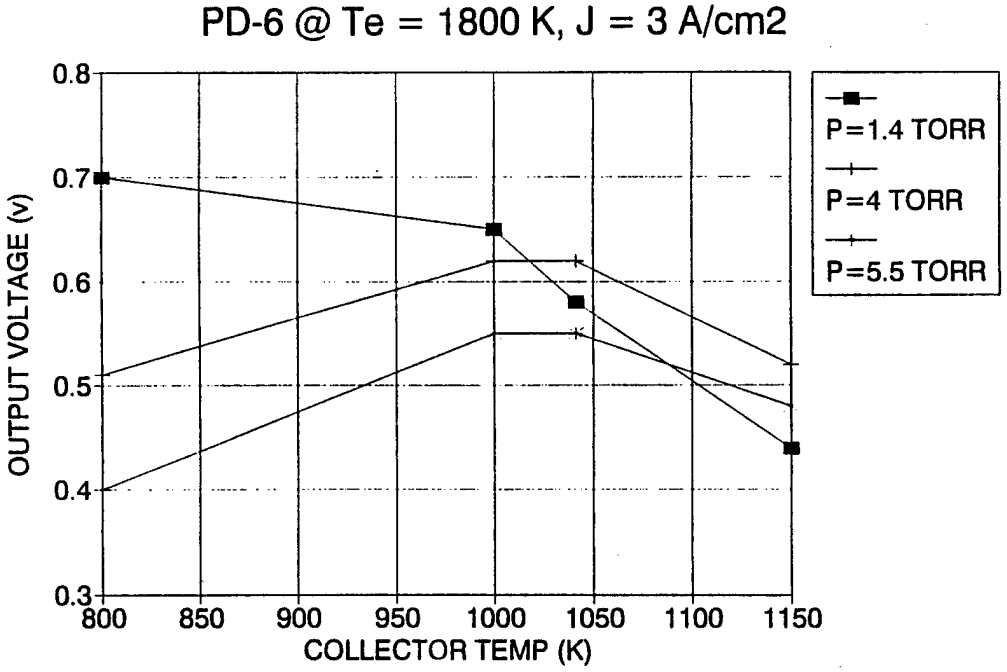

Figure 8-7 - Output voltage vs collector temperature

TFE-3H1 is different than the 1H series because the collector heater is replaced with a copper heat rejector to avoid high voltages required to operate long heater wires. The risks associated with collector heater failure with 3H and 6H devices were considered unacceptable. A significant portion of the temperature drop from the collector to the reactor water is taken between the collector and the copper heat conductor rather than between the collector heaters and the containment gas gaps. This design will be adjusted for 3H5 so that all collectors will run at about the same temperature.

References

8-1 TFE Verification Program Semiannual Report for the Period Ending September 30, 1991, GA-A20804, December 1991.

8-2 TFE Verification Program Semiannual Report for the Period Ending March 31, 1991, GA A20493, April 1991.

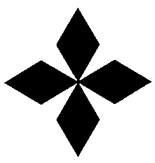

GENERAL ATOMICS

P. O. Box 85608 • San Diego, CA • 92186-9784 (619) 455-3000